

## APPENDIX: Lifetimes and timescales of tropospheric ozone

Michael J. Prather and Xin Zhu

### TABLES

Table A1. Chemistry in the UCI CTM

Table A2. Emissions & Boundary Conditions for these experiments

Table A3. UCI CTM References

### FIGURES

Figure A1. Stratospheric zonal mean O<sub>3</sub> abundance (ppm) averaged over four seasons (DJF, MAM, JJA, SON) comprised of 5-day snapshots from year 2003 of the CTRL run. Coordinates are latitude by pressure altitude  $z^* = 16 \text{ km} \log_{10}(1/P(\text{bars}))$  and assume a surface pressure everywhere of 1 bar.

Figure A2. Tropospheric zonal mean O<sub>3</sub> abundance (ppb), see Fig. A1. Some pixels in Fig. A1 and A2 contain both stratospheric and tropospheric values because the pixel contained was both stratospheric and tropospheric air over the 18 snapshots and 320 longitude cells (e.g., stratospheric intrusions).

Figure A3. Stratospheric (top) and tropospheric (bottom) global mean O<sub>3</sub> columns (DU) from the CTRL run calculated from the 365 5-day snapshots over the five years, 2000 through 2004.

Figure A4. Perturbation in the O<sub>3</sub> column (DU) for eO<sub>3</sub>avi (top), eO<sub>3</sub>srf (middle), and eO<sub>3</sub>ste1 (bottom), separating troposphere (blue) from stratosphere (red). Also shown are the decay of the perturbations following cessation of emissions on July 1 (2003.5) and Jan 1 (2004.0). In terms of DU, the annual emissions  $100 \text{ Tg-O}_3/\text{y} = 9.2 \text{ DU}/\text{y}$ , and thus a tropospheric perturbation of 0.5 DU has a lifetime of 20 days.

Figure A5. eO<sub>3</sub>avi perturbation to zonal mean O<sub>3</sub> abundance (ppb) for four seasons (DJF, MAM, JJA, SON), split into stratospheric (top panels) and tropospheric (bottom panels). For methodology, see Figure A1. Aviation emissions (eO<sub>3</sub>avi) occur mostly in the northern troposphere but reach into the stratosphere and southern hemisphere. Note that color bars have the same range on all plots.

Figure A6. eNO<sub>3</sub>avi perturbation to zonal mean O<sub>3</sub> abundance (ppb) for four seasons (DJF, MAM, JJA, SON), split into stratospheric (top panels) and tropospheric (bottom panels). For methodology, see Figure A1. For eNO<sub>3</sub>avi, aviation emissions of NO<sub>x</sub> are doubled. Note that color bars have the same range on all plots.

Figure A7. eO<sub>3</sub>srf perturbation to zonal mean O<sub>3</sub> abundance (ppb) for four seasons (DJF, MAM, JJA, SON), split into stratospheric (top panels) and tropospheric (bottom panels). For methodology, see Figure A1. Surface emissions (eO<sub>3</sub>srf) occur within the black square over a limited longitude range, see Table 1.

Figure A8. eO<sub>3</sub>ste1 perturbation to zonal mean O<sub>3</sub> abundance (ppb) for four seasons (DJF, MAM, JJA, SON), split into stratospheric (top panels) and tropospheric (bottom panels). For methodology, see Figure A1. STE emissions (eO<sub>3</sub>ste1) occur within the black squares equally in each hemisphere and across all longitudes, see Table 1.

Figure A9. eO3ste2 perturbation to zonal mean O<sub>3</sub> abundance (ppb) for four seasons (DJF, MAM, JJA, SON), split into stratospheric (top panels) and tropospheric (bottom panels). For methodology, see Figure A1. STE emissions (eO3ste2) occur within the black squares equally in each hemisphere and across all longitudes, see Table 1.

Figure A10. Stratospheric (top) and tropospheric (bottom) O<sub>3</sub> column (DU) for year 2003 from the control (CTRL) simulation. Columns are a function of latitude and time at 5-day intervals.

Figure A11. Ozone column perturbation (DU) for experiment eO3avi (aviation O<sub>3</sub>) as a function of latitude and time (2000.0 to 2004.0) at 5-day intervals for stratosphere (top) and troposphere (bottom).

Figure A12. Ozone column perturbation (DU) for experiment eNOavi (aviation NO<sub>x</sub>) as a function of latitude and time (2000.0 to 2004.0) at 5-day intervals for stratosphere (top) and troposphere (bottom).

Figure A13. Ozone column perturbation (DU) for experiment eO3srf (surface O<sub>3</sub>) as a function of latitude and time (2000.0 to 2004.0) at 5-day intervals for stratosphere (top) and troposphere (bottom).

Figure A14. Ozone column perturbation (DU) for experiment eO3ste1 (STE O<sub>3</sub>) as a function of latitude and time (2000.0 to 2004.0) at 5-day intervals for stratosphere (top) and troposphere (bottom).

Figure A15. Ozone column perturbation (DU) for experiment eO3ste2 (STE O<sub>3</sub>) as a function of latitude and time (2000.0 to 2004.0) at 5-day intervals for stratosphere (top) and troposphere (bottom).

Figure A16. Total (top) and tropospheric (bottom) burden of excess O<sub>3</sub> (Tg) for the five experiments, showing 5-day intervals for years 2000 through 2003. The spin up in early 2000 is clearly visible. The lifetime scale (days, right axis) is calculated from the emission rate of 100 Tg-O<sub>3</sub> yr<sup>-1</sup> for both tropospheric and total burden, and it does not apply to eNOavi (EO3B).

Figure A17. Burden of excess O<sub>3</sub> (Tg) for the five experiments: eO3avi (EO3A), eNOavi (EO3B), eO3ste1 (EO3T), eO3ste2 (EO3U), and eO3srf (EO3S). For each experiment, the tropospheric (dashed line), stratospheric (dotted line) and total (solid line) are shown. See Figure A16.

Figure A18. Instantaneous patterns of NH tropospheric O<sub>3</sub> perturbation for eO3avi/srf/ste1 at 1 Jul 2003 and 1 Jan 2004. All patterns are scaled to a total of 5 Tg.

Figure A19. (top) Decay of northern hemisphere tropospheric O<sub>3</sub> perturbations for eO3avi/srf/ste1 rescaled to 1 at the time of cessation of emission on July 1 (left) and January 1 (right). Dashed black lines are the same in both panels and show a constant decay of 10-, 20-, 30- and 40-day e-folds. The legend gives the min-to-max range in steady-state lifetime. Months are marked with vertical lines. (bottom) Same plot for southern hemisphere tropospheric O<sub>3</sub>.

Figure A20. Chemical mode patterns for the troposphere following decay of eO3avi/srf/ste1 starting at 1 Jul 2003 and 1 Jan 2004. Modes are calculated from averaged NH patterns after 1-2 months of decay (days 30-85). All perturbations are scaled to a total NH tropospheric O<sub>3</sub> perturbation of 5 Tg.

Figure A21. Latitude-by-altitude plots of the perturbations to key chemical species for the eO3avi (aviation) vs. CTRL on 1 Jul 2003. The upper-left-corner panel shows the O<sub>3</sub> perturbation in ppb to compare with earlier figures. All other panels, including the 2<sup>nd</sup> O<sub>3</sub> panel are in % difference. Note that the color bar, -3% to +3%, is the same for all the relative change panels.

**Table A1. Chemistry and Transport in the UCI CTM**

| <b>Tropospheric Chemical Species</b>   |  |                                 |   |   |  |  |                                   |
|--|--|---------------------------------|---|---|--|--|-----------------------------------|
| O( <sup>1</sup> D)*  | OH <sup>^</sup>  | O <sub>3</sub>                  | HO <sub>2</sub>   | NO  | NO <sub>2</sub>                            | NO <sub>3</sub>                                  | N <sub>2</sub> O <sub>5</sub>     |
| HNO <sub>3</sub>   | HNO <sub>4</sub>   | H <sub>2</sub> O <sub>2</sub>   | CH <sub>3</sub> OO  | CH <sub>3</sub> OOH                                       | H <sub>2</sub> CO                          | C <sub>2</sub> H <sub>5</sub> OO                 | C <sub>2</sub> H <sub>5</sub> OOH |
| C <sub>2</sub> H <sub>4</sub> O  | C <sub>2</sub> H <sub>3</sub> O <sub>3</sub>   | PAN                             | Alkene  | Alkane <sup>#</sup>                                       | C <sub>2</sub> H <sub>6</sub> <sup>#</sup> | CH <sub>4</sub> <sup>#</sup>                     | CO <sup>#</sup>                   |
| H <sub>2</sub> <sup>#</sup>  | C <sub>5</sub> H <sub>8</sub>  | C <sub>4</sub> H <sub>6</sub> O | C <sub>5</sub> H <sub>7</sub> O <sub>2</sub> <sup>^</sup> | C <sub>4</sub> H <sub>5</sub> O <sub>3</sub> <sup>^</sup> | ROHO <sub>2</sub> <sup>^</sup>             | C <sub>3</sub> H <sub>6</sub> O <sup>&amp;</sup> | H <sub>2</sub> O <sup>&amp;</sup> |
| e90 <sup>%</sup>   |  |                                 |   |   |  |  |                                   |
| All species included as implicit chemistry and transport EXCEPT: * = instant steady state; ^ = transported with +parent molecule (see below); # = explicit chemistry; & = specified abundance; % = no chemistry, 90-day e-fold.  |  |                                 |   |   |  |  |                                   |
| Key: C <sub>2</sub> H <sub>4</sub> O = Acetaldehyde; C <sub>2</sub> H <sub>3</sub> O <sub>3</sub> = Peroxyacetyl radical; PAN = C <sub>2</sub> H <sub>3</sub> O <sub>3</sub> NO <sub>2</sub> = Peroxyacetyl nitrate; Alkene = C <sub>3</sub> H <sub>6</sub> + other alkene emissions; Alkane = C <sub>3</sub> H <sub>8</sub> + higher alkane emissions; C <sub>5</sub> H <sub>8</sub> = Isoprene; C <sub>4</sub> H <sub>6</sub> O = Methacrolein or Methyl vinyl ketone; C <sub>5</sub> H <sub>7</sub> O <sub>2</sub> = Isoprene peroxy radical (all types); C <sub>4</sub> H <sub>5</sub> O <sub>3</sub> = Methyl vinyl ketone peroxy radicals (all types); ROHO <sub>2</sub> = C <sub>3</sub> H <sub>7</sub> O <sub>3</sub> = Hydroxypropanyl peroxy radical formed from Alkene + OH; C <sub>3</sub> H <sub>6</sub> O = Acetone. |  |                                 |   |   |  |  |                                   |
| Transported pairs, for the chemistry initialize: OH as 1% of HO <sub>2</sub> ; ROHO <sub>2</sub> as 0.1% of Alkene; C <sub>5</sub> H <sub>7</sub> O <sub>2</sub> as 0.1% of C <sub>5</sub> H <sub>8</sub> ; C <sub>4</sub> H <sub>5</sub> O <sub>3</sub> as 0.1% of C <sub>4</sub> H <sub>6</sub> O.   |  |                                 |   |   |  |  |                                   |
| <b>Stratospheric Chemical Species</b>  |  |                                 |   |   |  |  |                                   |
| O <sub>3</sub>   | N <sub>2</sub> O   | CH <sub>4</sub>                 | NO <sub>y</sub>   |   |  |  |                                   |
| Notes: NO <sub>y</sub> = NO + NO <sub>2</sub> + NO <sub>3</sub> + 2 N <sub>2</sub> O <sub>5</sub> + HNO <sub>3</sub> + HNO <sub>4</sub> + PAN  |  |                                 |   |   |  |  |                                   |
| <b>Tracer Transport</b>  |  |                                 |   |   |  |  |                                   |
| source   | ECMWF IFS cycle 38r1 3-hr averaged forecasts (winds, convection, temperature, q, rain, clouds)   |                                 |   |   |  |  |                                   |
| resolution   | native resolution T159L60 (1.1° x 1.1°, 34 layers in troposphere)                                |                                 |   |   |  |  |                                   |
| numerics   | second-order moments for tracers, fractional overlap for clouds and washout, explicit STE fluxes |                                 |   |   |  |  |                                   |

**Table A2. Emissions & Boundary Conditions**

| Species                         | Tg-species per year | Notes  |
|---------------------------------|---------------------|--|
| NO                              | 88.2 + 10.7         | Lightning NO <sub>x</sub> tuned to 5 TgN = 10.7 TgNO as multi-year average |
| NO <sub>2</sub>                 | 0.1                 |  |
| H <sub>2</sub> CO               | 14.4                |  |
| CO                              | 1274.4              |  |
| C <sub>2</sub> H <sub>6</sub>   | 7.8                 |  |
| C <sub>2</sub> H <sub>4</sub> O | 23.5                |  |
| Alkane                          | 49.1                |  |
| Alkene                          | 66.9                |  |
| Isoprene                        | 523.4               |  |
| e90                             | 2073.8              | Globally uniform surface, tuned to give 100 ppb at steady state            |

| Emission Source           | Reference           | Species  |
|---------------------------|---------------------|--|
| Anthropogenic surface     | RCP 6.0 year 2000   | NO, CO, C <sub>2</sub> H <sub>6</sub> , Alkane, Alkene, H <sub>2</sub> CO, C <sub>2</sub> H <sub>4</sub> O |
| Aviation NO <sub>x</sub>  | RCP 6.0 year 2000   | NO (96%), NO <sub>2</sub> (4%)   |
| Biomass burning           | GFED4 year 1997     | NO, CO, C <sub>2</sub> H <sub>6</sub> , Alkane, Alkene, H <sub>2</sub> CO, C <sub>2</sub> H <sub>4</sub> O |
| Biogenics                 | MEGAN 2.1           | CO, Alkene, H <sub>2</sub> CO, C <sub>2</sub> H <sub>4</sub> O, C <sub>5</sub> H <sub>8</sub>              |
| Lightning NO <sub>x</sub> | Holmes++ 2013, 2104 | NO   |

| Species                         | Fixed abundance  | Notes   |
|---------------------------------|--|---|
| CH <sub>4</sub>                 | LBC: SH-NH = 1750-1850 ppb   |   |
| N <sub>2</sub> O                | LBC: SH-NH = 316-316 ppb   |   |
| H <sub>2</sub>                  | LBC: SH-NH = 550-500 ppb   |   |
| C <sub>3</sub> H <sub>6</sub> O | All trop: 90S-60S-30S-20S-20N-30N-60N-90N<br>= 150-250-350-500-700-900-700 ppt | From ATom, uniform in vertical<br>= 200-200-200-400-600-600-600 ppt |

**Table A3. UCI CTM References** documenting application and development of UCI CTM and its components. This chemistry-transport model began as a Harvard & GISS joint enterprise, and then moved to UC Irvine. The meteorological fields used in the CTM were originally from the GISS GCM developed by Gary Russell (11-layer tropospheric model and 21-layer stratospheric model). In the late 1990s Jostein Sundet visited UCI and developed the next generation of meteorological fields based on the ECMWF IFS that U. Oslo had access to. The tropospheric chemistry was initially built by Oliver Wild while at FRSGC Yokohama and thus also known as FRSGC CTM. After 1992, most all of the lead authors on these papers were graduate students, post-docs, or visitors in the Earth System Science Department at UC Irvine.

1. Sand, Maria, R. B. Skeie, M. Sandstad, S. Krishnan, G. Myhre, H. Bryant, R. Derwent, D. Hauglustaine, F. Paulot, M. Prather & D. Stevenson (2023) A multi-model assessment of the Global Warming Potential of hydrogen, *Nature Communications: Earth & Environment*, 4:203, doi: 10.1038/s43247-023-00857-8.
2. Prather, M. J. (2022) CO<sub>2</sub> surface variability: from the stratosphere or not?, *Earth Syst. Dynam.*, 13, 703–709, doi: 10.5194/esd-13-703-2022.
3. Ruiz, D. J. and M.J. Prather (2022) From the middle stratosphere to the surface, using nitrous oxide to constrain the stratosphere–troposphere exchange of ozone, *Atmos. Chem. Phys.*, 22, 2079–2093, doi: 10.5194/acp-22-2079-2022.
4. Ruiz, Daniel J., Michael J. Prather, Susan E. Strahan, Rona L. Thompson, Lucien Froidevaux, Stephen D. Steenrod (2021), How atmospheric chemistry and transport drive surface variability of N<sub>2</sub>O and CFC-11. *J. Geophys. Res.: Atmospheres*, 126, e2020JD033979, doi: 10.1029/2020JD033979.
5. Nicewonger, M. R., Aydin, M., Prather, M. J., & Saltzman, E. S. (2020). Extracting a history of global fire emissions for the past millennium from ice core acetylene, ethane, and methane, *J. Geophys. Res.-Atmos.* 125 (20), e2020JD032932.
6. Nicewonger, M. R., Aydin, M., Prather, M. J., & Saltzman, E. S. (2020). Reconstruction of paleofire emissions over the past millennium from measurements of ice core acetylene. *Geophysical Research Letters*, 47, e2019GL085101. doi.org/10.1029/2019GL085101.
7. Prather, M.J. and J.C. Hsu (2019) A round Earth for climate models, *Proc Natl Acad Sci*, 116 (39) 19330–19335; <https://doi.org/10.1073/pnas.1908198116>.
8. Nicewonger, M.R., M. Aydin, M.J. Prather, E.S. Saltzman, (2018) Large changes in biomass burning over the last millennium inferred from paleoatmospheric ethane in polar ice cores, *PNAS*, 115 (49), 12413–12418, doi: 10.1073/pnas.1807172115.
9. Hall, Samuel R., Kirk Ullmann, Michael J. Prather, Clare M. Flynn, Lee T. Murray, Arlene M. Fiore, Gustavo Correa, Sarah A. Strode, Stephen D. Steenrod, Jean-Francois Lamarque, Jonathon Guth, Béatrice Josse, Johannes Flemming, Vincent Huijnen, N. Luke Abraham, and Alex T. Archibald (2018) Cloud impacts on photochemistry: a new climatology of photolysis rates from the Atmospheric Tomography mission, *Atmos. Chem. Phys.*, 18, 16809–16828, doi: 10.5194/acp-18-16809-2018.
10. Prather, M.J., Clare M. Flynn, Xin Zhu, Stephen D. Steenrod, Sarah A. Strode, Arlene M. Fiore, Gustavo Correa, Lee T. Murray, and Jean-Francois Lamarque (2018) How well can global chemistry models calculate the reactivity of short-lived greenhouse gases in the remote troposphere, knowing the chemical composition, *Atmos. Meas. Tech.*, 11, 2653–2668, 2018, doi: 10.5194/amt-11-2653-2018.
11. Prather, M.J., Xin Zhu, Clare M. Flynn, Sarah A. Strode, Jose M. Rodriguez, Stephen D. Steenrod, Junhua Liu, Jean-Francois Lamarque, Arlene M. Fiore, Larry W. Horowitz, Jingqiu Mao, Lee T. Murray, Drew T. Shindell, and Steven C. Wofsy (2017) Global Atmospheric Chemistry – Which Air Matters, *Atmos. Chem. Phys.*, 17(14), 9081–9102, doi: 10.5194/acp-17-9081-2017.
12. Prather, M.J. (2015) Photolysis rates in correlated overlapping cloud fields: Cloud-J 7.3c, *Geosci. Model Dev.*, 8, 2587–2595, doi:10.5194/gmd-8-2587-2015.
13. Prather, M.J., J. Hsu, N.M. DeLuca, C.H. Jackman, L.D. Oman, A.R. Douglass, E.L. Fleming, S.E. Strahan, S.D. Steenrod, O.A. Søvde, I.S.A. Isaksen, L. Froidevaux, and B. Funke (2015) Measuring and modeling the lifetime of nitrous oxide including its variability, *J. Geophys. Res. Atmos.*, 120, 5693–5705. doi: 10.1002/2015JD023267.

14. Hsu, Juno and M.J. Prather (2014) Is the vertical residual velocity a good proxy for stratosphere-troposphere exchange of ozone? *Geophys. Res. Lett.*, 41, doi:10.1029/2014GL061994
15. Schnell, J.L., C. D. Holmes, A. Jangam, M. J. Prather (2014) Skill in forecasting extreme ozone pollution episodes with a global atmospheric chemistry model, *Atmos. Chem. Phys.*, 14, 7721–7739, doi:10.5194/acp-14-7721-2014.
16. Holmes, C.D., M. J. Prather, and G. C. M. Vinken (2014) The climate impact of ship NO<sub>x</sub> emissions: an improved estimate accounting for plume chemistry, *Atmos. Chem. Phys.*, 14, 6801–6812, doi:10.5194/acp-14-6801-2014
17. Lauritzen, P.H., P.A. Ullrich, C. Jablonowski, P. A. Bosler, D. Calhoun, A.J. Conley, T. Enomoto, L. Dong, S. Dubey, O. Guba, A.B. Hansen, E. Kaas, J. Kent, J.-F. Lamarque, M.J. Prather, D. Reinert, V.V. Shashkin, W.C. Skamarock, B. Sørensen, M.A. Taylor, and M.A. Tolstykh (2014) A standard test case suite for two-dimensional linear transport on the sphere: results from a collection of state-of-the-art schemes, *Geosci. Model Dev.*, 7, 105–145, doi:10.5194/gmd-7-105-2014.
18. Hsu, Juno, M.J. Prather, D. Bergmann, P. Cameron-Smith (2013), Sensitivity of stratospheric dynamics to uncertainty in O<sub>3</sub> production, *J. Geophys. Res. Atmos.*, 118, 8984–8999, doi:10.1002/jgrd.50689.
19. Holmes, C.D., M. J. Prather, A.O. Søvde, G. Myhre (2013) Future methane, hydroxyl, and their uncertainties: key climate and emission parameters for future predictions, *Atmos. Chem. Phys.*, 13, 285–302, doi:10.5194/acp-13-285-2013
20. Tang, Qi and M. J. Prather (2012), Tropospheric column ozone: matching individual profiles from Aura OMI and TES with a chemistry-transport model, *Atmos. Chem. Phys.*, 12, 10441-10452, doi:10.5194/acp-12-10441-2012.
21. Tang, Qi and M.J. Prather (2012), Five blind men and the elephant: what can the NASA Aura ozone measurements tell us about stratosphere-troposphere exchange? *Atmos. Chem. Phys.*, 12, 2357–2380, doi:10.5194/acp-12-2357-2012.
22. Neu, J.L. and M. J. Prather (2012), Toward a more physical representation of precipitation scavenging in global chemistry models: cloud overlap and ice physics and their impact on tropospheric ozone, *Atmos. Chem. Phys.*, 12, 3289-3310, doi:10.5194/acp-12-3289-2012.
23. Holmes, C.D., Q. Tang, M.J. Prather (2011) Uncertainties in climate assessment: the case of aviation NO<sub>x</sub>, *PNAS*, 108(27): 10997-11002, doi: 10.1073/pnas.1101458108.
24. Prather, M.J., X. Zhu, Q. Tang, J. Hsu, J.L. Neu (2011), An atmospheric chemist in search of the tropopause, *J. Geophys. Res.*, 116: D04306, doi:10.1029/2010JD014939.
25. Tang, Qi, M.J. Prather, J. Hsu (2011), Stratosphere-troposphere exchange ozone flux related to deep convection, *Geophys. Res. Lett.*, 38: L03806, doi:10.1029/2010GL046039.
26. PhotoComp (2010), Chapter 6 in SPARC CCMVal Report on Evaluation of Chemistry-Climate Models (V. Eyring, T. G. Shepherd, D. W. Waugh, eds.), SPARC Report No. 5, WCRP-30/2010, WMO/TD – No. 40, [www.sparc-climate.org/publications/sparc-reports/](http://www.sparc-climate.org/publications/sparc-reports/).
27. Prather, M.J. and J. Hsu (2010), Coupling of nitrous oxide and methane by global atmospheric chemistry, *Science*, 330: 952-954.
28. Tang, Qi and M.J. Prather (2010), Correlating tropospheric column ozone with tropopause folds: the Aura-OMI satellite data, *Atmos. Chem. Phys.*, 10, 9581-9688.
29. Hsu, Juno and M. J. Prather (2010), Global long-lived chemical modes excited in a 3-D chemistry transport model: Stratospheric N<sub>2</sub>O, NO<sub>y</sub>, O<sub>3</sub> and CH<sub>4</sub> chemistry, *Geophys. Res. Lett.*, 37, L07805, doi:10.1029/2009GL042243.
30. Prather, M. J. (2009), Tropospheric O<sub>3</sub> from photolysis of O<sub>2</sub>, *Geophys. Res. Lett.*, 36, L03811, doi:10.1029/2008GL036851
31. Hsu, J., M. J. Prather (2009), Stratospheric variability and tropospheric ozone, *J. Geophys. Res.*, 114, D06102, doi: 10.1029/2008JD010942
32. Prather M.J., X. Zhu, S.E. Strahan, S.D. Steenrod, J.M. Rodriguez (2008), Quantifying errors in trace species transport modeling, *Proc. Nat. Acad. Sci.* 105(50): 19617-19621.
33. Neu J. L., M. J. Lawler, M. J. Prather, E. S. Saltzman (2008), Oceanic alkyl nitrates as a natural source of tropospheric ozone, *Geophys. Res. Lett.*, 35: L13814.

34. Neu, J.L., M.J. Prather, J.E. Penner (2007) Global atmospheric chemistry: integrating over fractional cloud cover, *J. Geophys. Res.*, 112, D11306.
35. Wild, O. and M.J. Prather (2006) Global tropospheric ozone modeling: Quantifying errors due to grid resolution, *J. Geophys. Res.*, 111(D11), D11305, doi:10.1029/2005JD006605.
36. Hsu, J., M. J. Prather, and O. Wild (2005), Diagnosing the stratosphere-to-troposphere flux of ozone in a chemistry transport model, *J. Geophys. Res.*, 110, D19305, doi:10.1029/2005JD006045.
37. Marandino, C. A., W. J. De Bruyn, S. D. Miller, M. J. Prather, and E. S. Saltzman (2005), Oceanic uptake and the global atmospheric acetone budget, *Geophys. Res. Lett.*, 32, L15806, doi:10.1029/2005GL023285. [see Correction, *GRL* 33(24): Art. No. L24801, 2006.]
38. Ehhalt, D. H., F. Rohrer, S. Schauffler, M. J. Prather (2004) On the decay of stratospheric pollutants: diagnosing the longest-lived eigenmode, *J. Geophys. Res.*, 109(D8), D08102 10.1029/2003JD004029.
39. Wild, Oliver, M. J. Prather, H. Akimoto, J. K. Sundet, I. S. A. Isaksen, J. H. Crawford, D. D. Davis, M. A. Avery, Y. Kondo, G. W. Sachse, S. T. Sandholm (2004) Chemical transport model ozone simulations for spring 2001 over the western Pacific: Regional ozone production and its global impacts, *J. Geophys. Res.*, 109(D15), D15S02, doi:10.1029/2003JD004041.
40. Hsu, Juno, M. J. Prather, O. Wild, J.K. Sundet, I.S.A. Isaksen, E.V. Browell, M.A. Avery, G.W. Sachse (2004) Are the TRACE-P measurements representative of the Western Pacific during March 2001? *J. Geophys. Res.*, 109(D02 314), doi:10.1029/2003JD004002.
41. Wild, O., J.K. Sundet, M.J. Prather, I.S.A. Isaksen, H. Akimoto, E.V. Browell, and S.J. Oltmans (2003) CTM Ozone Simulations for Spring 2001 over the Western Pacific: Comparisons with TRACE-P lidar, ozonesondes and TOMS columns, *J. Geophys. Res.*, 108(D21), 8826, doi:10.1029/2002JD003283.
42. McLinden, C. A., M. J. Prather, M. S. Johnson (2003) Global modeling of the isotopic analogues of N<sub>2</sub>O: Stratospheric distributions, budgets, and the 17O–18O mass-independent anomaly, *J. Geophys. Res.*, 108(D8), 4233, doi:10.1029/2002JD002560.
43. Bian, H., M. J. Prather, and T. Takemura (2003) Tropospheric aerosol impacts on trace gas budgets through photolysis, *J. Geophys. Res.*, 108(D8), 4242, doi:10.1029/2002JD002743.
44. Johnston, N. A. C., J. J. Colman, D. R. Blake, M. J. Prather, and F. S. Rowland (2002) On the variability of tropospheric gases: Sampling, loss patterns, and lifetime, *J. Geophys. Res.*, 107(D11), 4111, doi:10.1029/2001JD000669.
45. Bian, H., and M.J. Prather (2002) Fast-J2: Accurate Simulation of stratospheric photolysis in global chemical models, *J. Atmos. Chem.*, 41, 281-296.
46. Gurney K.R., Law R.M., Denning A.S., Rayner P.J., Baker D., Bousquet P., Bruhwiler L., Chen Y.H., Ciais P., Fan S, Fung IY, Gloor M, Heimann M, Higuchi K, John J, Maki T, Maksyutov S, Masarie K, Peylin P, Prather M, Pak BC, Randerson J, Sarmiento J, Taguchi S, Takahashi T, Yuen CW (2002) Towards robust regional estimates of CO<sub>2</sub> sources and sinks using atmospheric transport models, *Nature*, 415, 626-630.
47. Pak, B.C., and M.J. Prather (2001) CO<sub>2</sub> source inversions using satellite observations of the upper troposphere, *Geophys. Res. Lett.*, 28, 4571-4574.
48. Olsen, S. C., C. A. McLinden, and M. J. Prather (2001) The Stratospheric NO<sub>y</sub>-N<sub>2</sub>O System: Testing uncertainties in a 3-D framework, *J. Geophys. Res.*, 106(D22), 28771-28784.
49. Wild, O., M. J. Prather, H. Akimoto (2001) Indirect long-term global cooling from NO<sub>x</sub> emissions, *Geophys. Res. Lett.*, 28, 1719-1722, doi: 10.1029/2000GL012573.
50. Wild, O. and M.J. Prather (2000) Excitation of the primary tropospheric chemical mode in a global three-dimensional model, *J. Geophys. Res.*, 105, 24647-24660.
51. McLinden, C., S. Olsen, B. Hannegan, O. Wild, M. Prather, and J. Sundet (2000) Stratospheric ozone in 3-D models: a simple chemistry and the cross-tropopause flux, *J. Geophys. Res.*, 105, 14653-14665.
52. Wild, O., X. Zhu, and M.J. Prather (2000) Fast-J: Accurate simulation of in- and below-cloud photolysis in tropospheric chemical models, *J. Atmos. Chem.*, 37, 245-282.
53. Olsen, S.C., B. J. Hannegan, X. Zhu, and M.J. Prather (2000) Evaluating ozone depletion from very short-lived halocarbons, *Geophys. Res. Lett.*, 27, 1475-1478.
54. Hall, T.M., D.W. Waugh, K.A. Boering, R.A. Plumb (1999) Evaluation of transport in stratospheric models, *J. Geophys. Res.* 104, 18815-18139, doi: 10.1029/1999JD900226.

55. Hannegan, B. S. Olsen, M. Prather, X. Zhu, D. Rind, and J. Lerner (1998) The dry stratosphere: A limit on cometary water influx, *Geophys. Res. Lett.*, 25, 1649-1652.
56. Ehhalt, D.H., F. Rohrer, A. Wahner, M.J. Prather, and D.R. Blake (1998) On the use of hydrocarbons for the determination of tropospheric OH concentrations, *J. Geophys. Res.* 103, 18981-18997.
57. Avallone, L.M. and M.J. Prather (1997) Tracer-tracer correlations: three-dimensional model simulations and comparisons to observations, *J. Geophys. Res.*, 102, 19233-19246.
58. Ehhalt, D.H., F. Rohrer, A.B. Kraus, M.J. Prather, D.R. Blake, and F.S. Rowland (1997) On the significance of regional trace gas distributions as derived from aircraft campaigns in PEM-West A and B, *J. Geophys. Res.* 102, 28333-28351.
59. Hall, T.M. & M.J. Prather (1995) Seasonal evolution of N<sub>2</sub>O, O<sub>3</sub>, and CO<sub>2</sub>: three-dimensional simulations of stratospheric correlations, *J. Geophys. Res.*, 100, 16699-16720.
60. Hall, T.M., & M.J. Prather (1993) Simulations of the Trend and Annual Cycle in Stratospheric CO<sub>2</sub>, *J. Geophys. Res.*, 98, 10573-10581.
61. Fung, I., J. John, J. Lerner, E. Matthews, M. Prather, L.P. Steele and P.J. Fraser (1991) Three-Dimensional Model Synthesis of the Global Methane Cycle, *J. Geophys. Res.*, 96, 13,033-13,065.
62. Jacob, D.J. and M.J. Prather (1990) Radon-222 as a test of the boundary-layer convection in a general circulation model, *Tellus* 42B, 118-134.
63. Prather, M., M.M. Garcia, R. Suozzo and D. Rind (1990) Global impact of the Antarctic ozone hole: dynamical dilution with a 3-D chemical transport model, *J. Geophys. Res.* 95, 3449-3471.
64. Prather, M.J. & J.M. Rodriguez (1988) Antarctic ozone: meteoric control of HNO<sub>3</sub>, *Geophys. Res. Lett.* 15, 1-4, doi: 10.1029/GL015i001p00001.
65. Prather, M., M. McElroy, S. Wofsy, G. Russell and D. Rind (1987) Chemistry of the global troposphere: fluorocarbons as tracers of air motion, *J. Geophys. Res.* 92, 6579-6613.
66. Prather, M.J. (1986) Numerical advection by conservation of second-order moments. *J. Geophys. Res.* 91, 6671-6681, doi: 10.1029/JD091iD06p06671

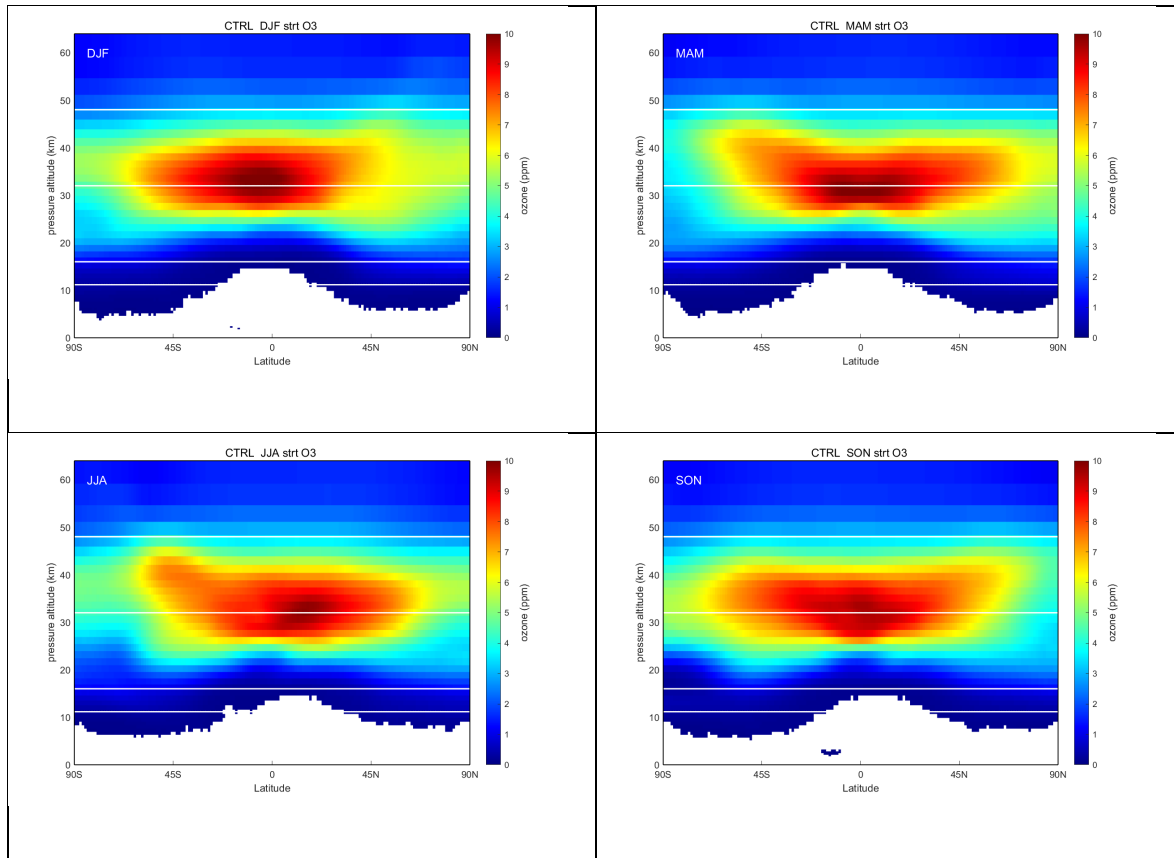


**Figure A1. Stratospheric zonal mean O<sub>3</sub> abundance (ppm) averaged over four seasons (DJF, MAM, JJA, SON) comprised of 5-day snapshots from year 2003 of the CTRL run. Coordinates are latitude by pressure altitude  $z^* = 16 \text{ km} \log_{10}(1/P(\text{bars}))$  and assume a surface pressure everywhere of 1 bar.**

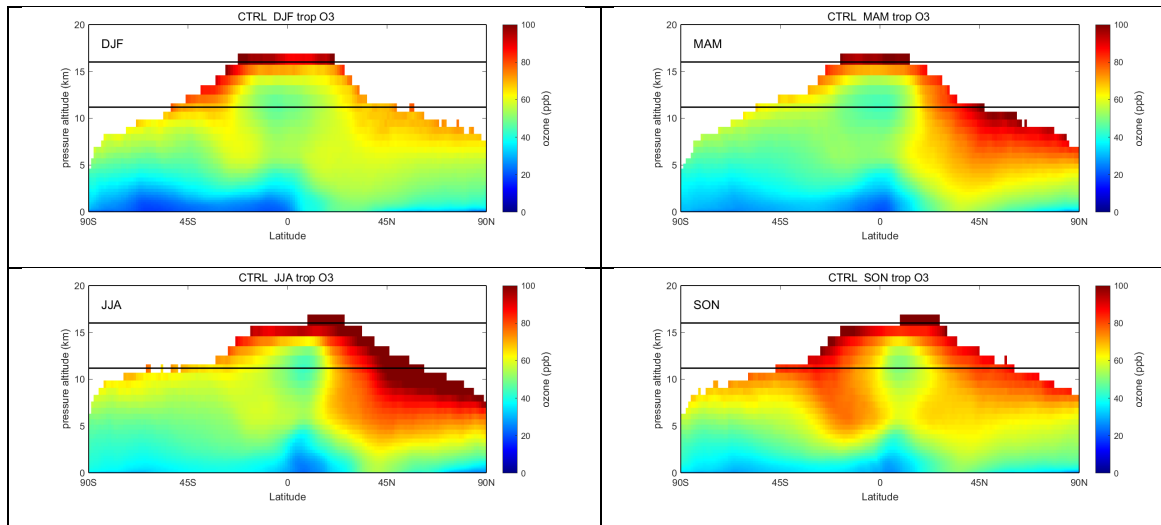


**Figure A2. Tropospheric zonal mean O<sub>3</sub> abundance (ppb), see Fig. A1. Some pixels in Fig. A1 and A2 contain both stratospheric and tropospheric values because the pixel contained was both stratospheric and tropospheric air over the 18 snapshots and 320 longitude cells (e.g., stratospheric intrusions).**

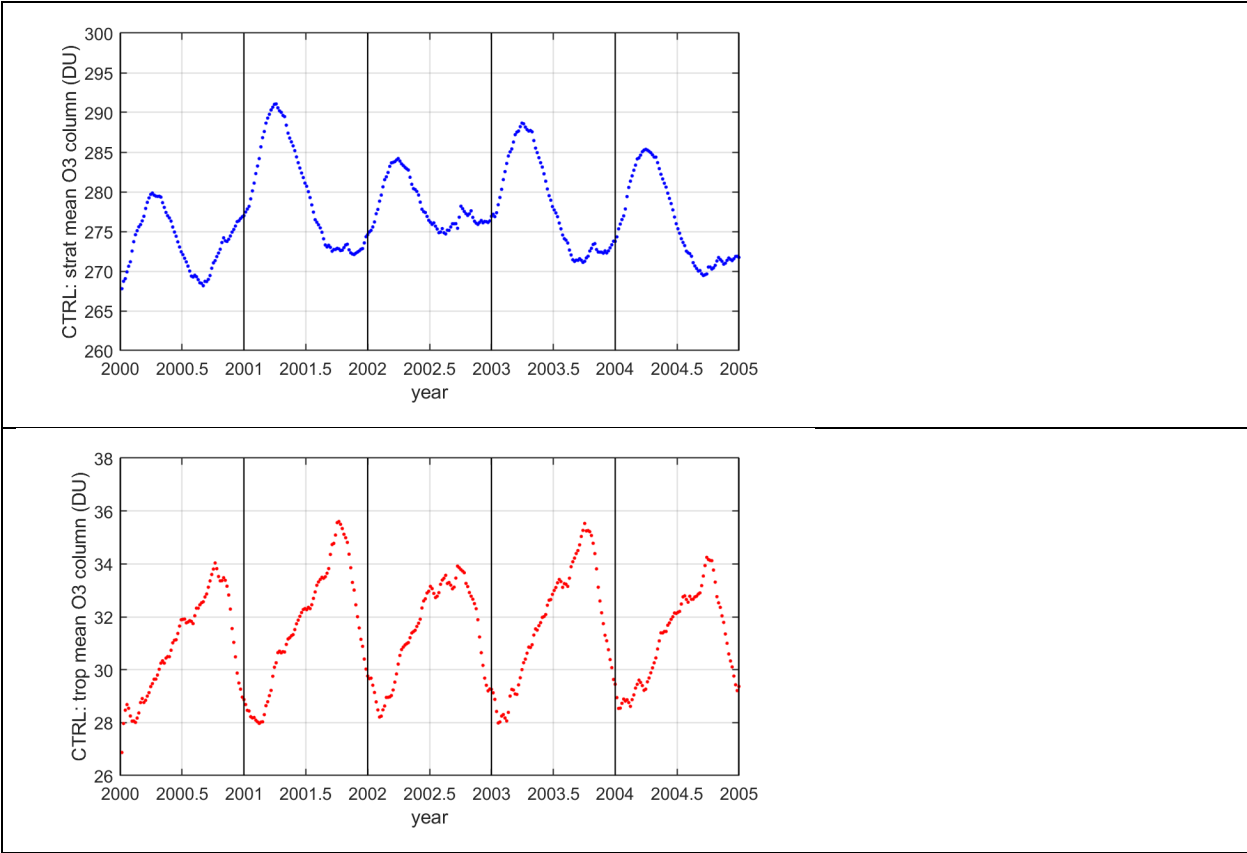


**Figure A3. Stratospheric (top) and tropospheric (bottom) global mean O<sub>3</sub> columns (DU) from the CTRL run calculated from the 365 5-day snapshots over the five years, 2000 through 2004.**

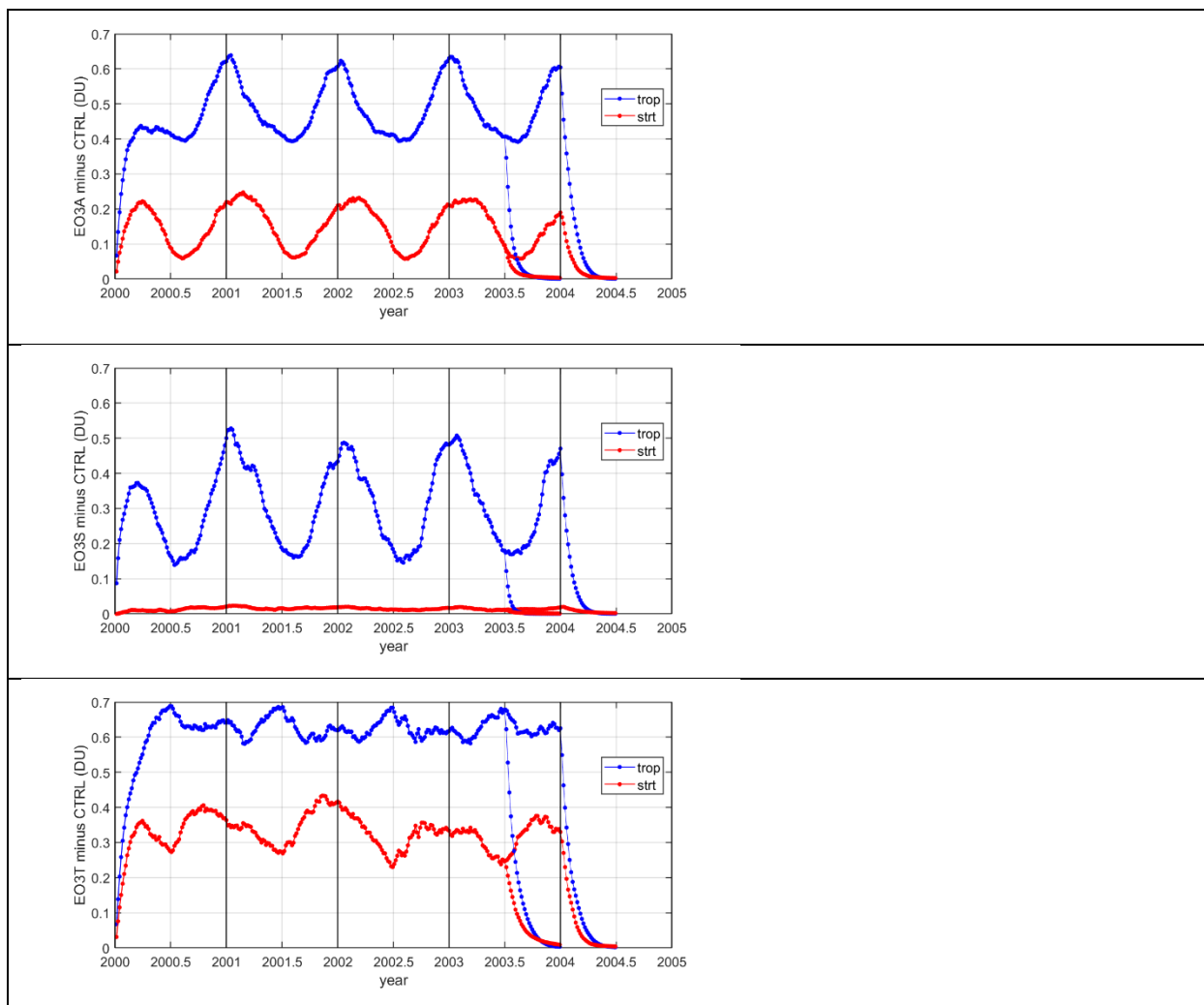


**Figure A4. Perturbation in the O<sub>3</sub> column (DU) for eO3avi (EO3A, top), eO3srf (EO3S, middle), and eO3stel (EO3T, bottom), separating troposphere (blue) from stratosphere (red). Also shown are the decay of the perturbations following cessation of emissions on July 1 (2003.5) and Jan 1 (2004.0). In terms of DU, the annual emissions are about 9.2 DU, and thus a tropospheric perturbation of 0.4 DU has a lifetime of 16 days.**

## eO3avi (EO3A)

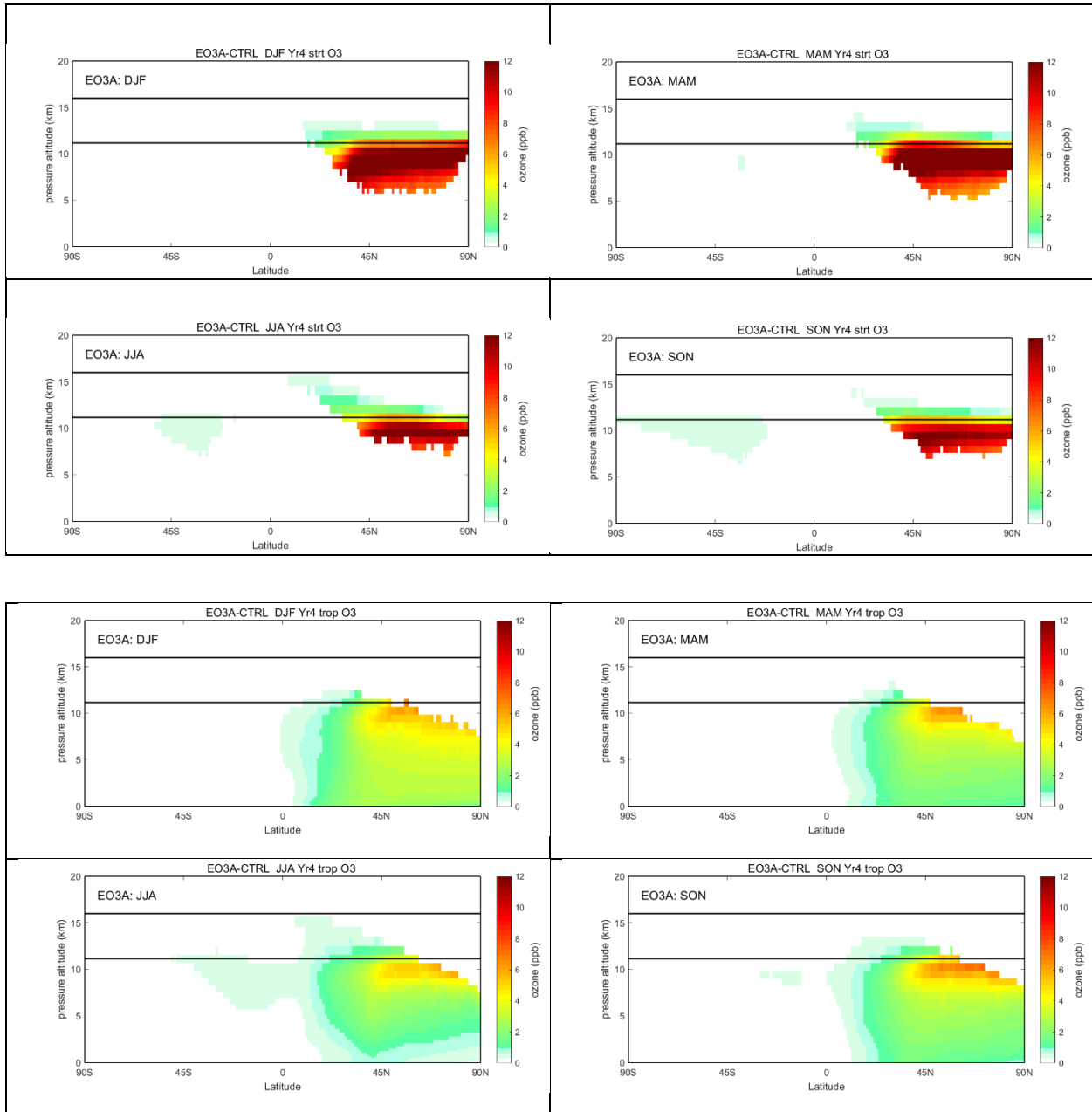


**Figure A5.** eO3avi perturbation to zonal mean O<sub>3</sub> abundance (ppb) for four seasons (DJF, MAM, JJA, SON), split into stratospheric (top panels) and tropospheric (bottom panels). For methodology, see Figure A1. Aviation emissions (eO3avi) occur mostly in the northern troposphere but reach into the stratosphere and southern hemisphere. Note that color bars have the same range on all plots.

## eNOavi (EO3B)

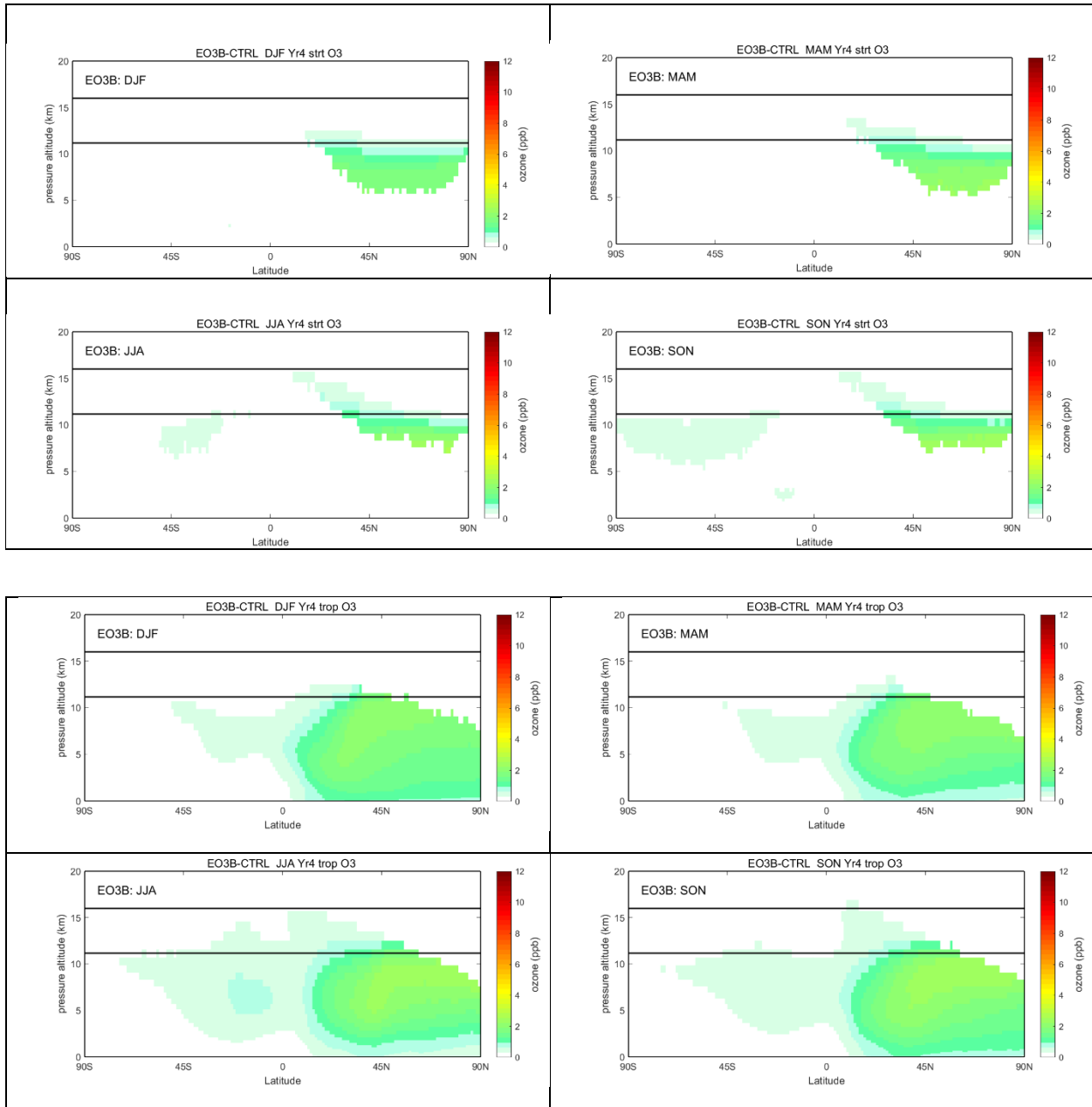


**Figure A6. eNOavi perturbation to zonal mean O<sub>3</sub> abundance (ppb) for four seasons (DJF, MAM, JJA, SON), split into stratospheric (top panels) and tropospheric (bottom panels). For methodology, see Figure A1. Aviation emissions (eNOavi) occur as NO<sub>x</sub>. Note that color bars have the same range on all plots.**

## eO3srf (EO3S)

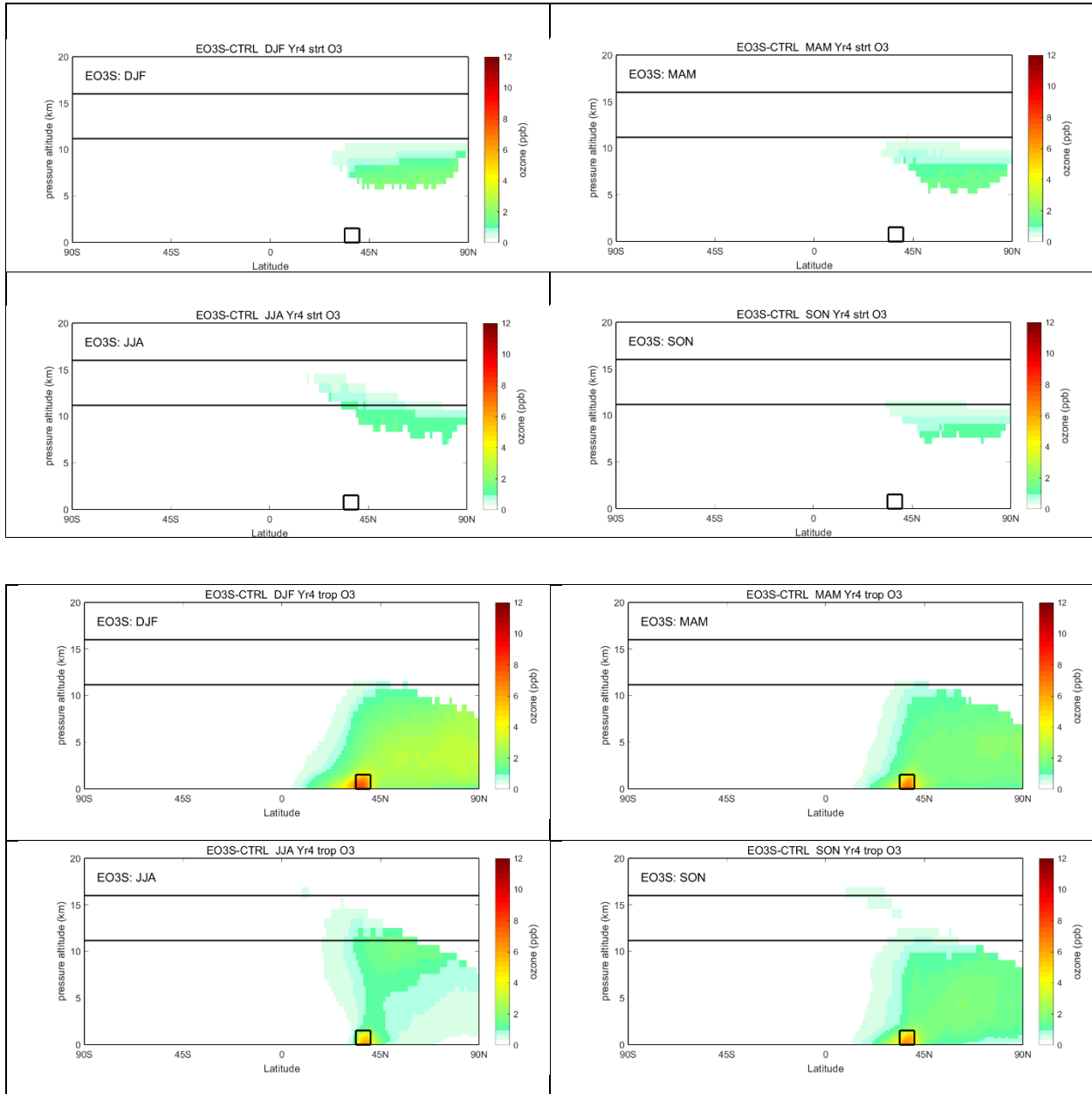


**Figure A7. eO3srf perturbation to zonal mean O<sub>3</sub> abundance (ppb) for four seasons (DJF, MAM, JJA, SON), split into stratospheric (top panels) and tropospheric (bottom panels). For methodology, see Figure A1. Surface emissions (eO3srf) occur within the black square over a limited longitude range, see Table 1.**

## eO3ste1 (EO3T)

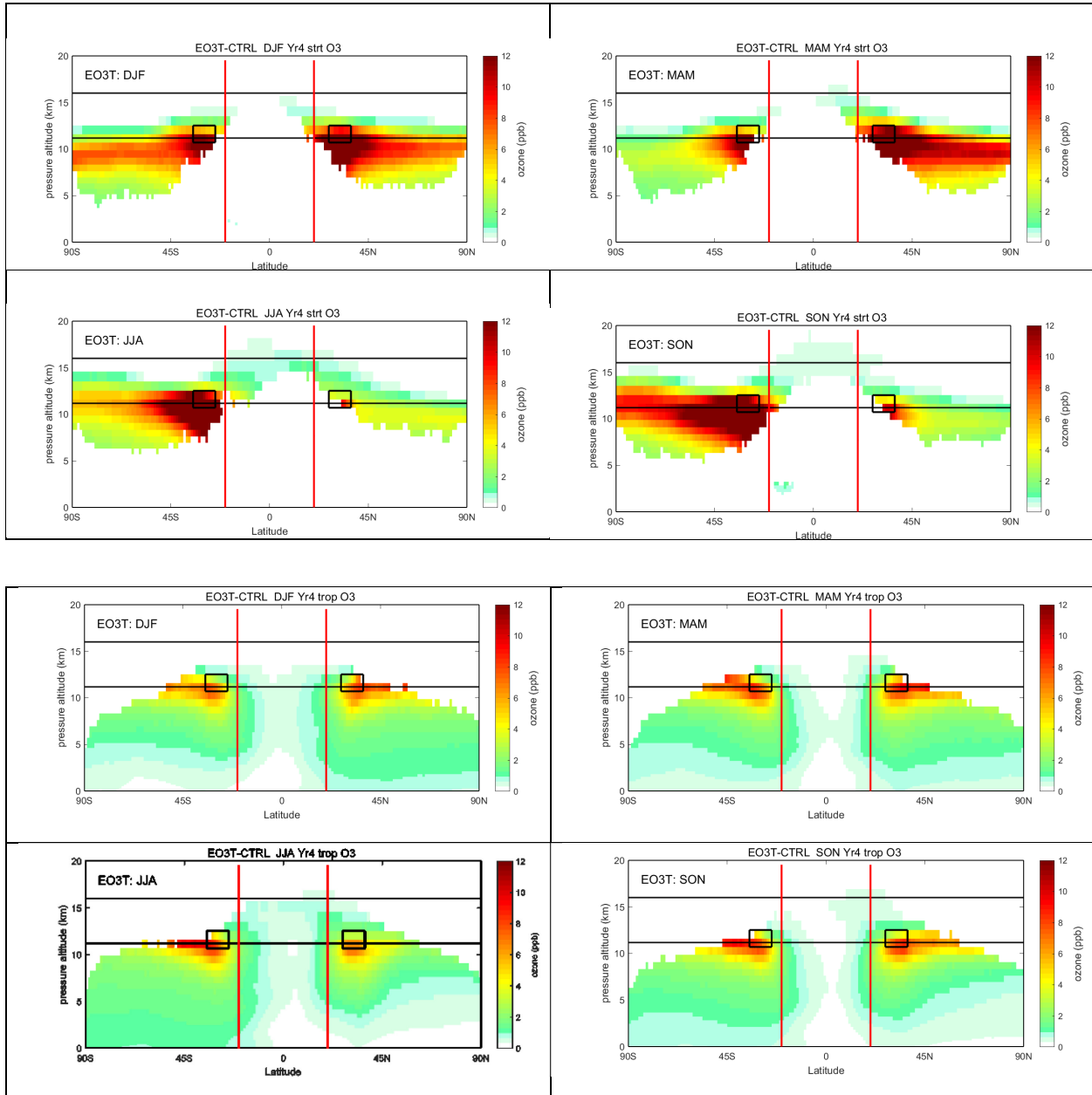


**Figure A8.** eO3ste1 perturbation to zonal mean O<sub>3</sub> abundance (ppb) for four seasons (DJF, MAM, JJA, SON), split into stratospheric (top panels) and tropospheric (bottom panels). For methodology, see Figure A1. STE emissions (eO3ste1) occur within the black squares equally in each hemisphere and across all longitudes, see Table 1.

## eO3ste2 (EO3U)

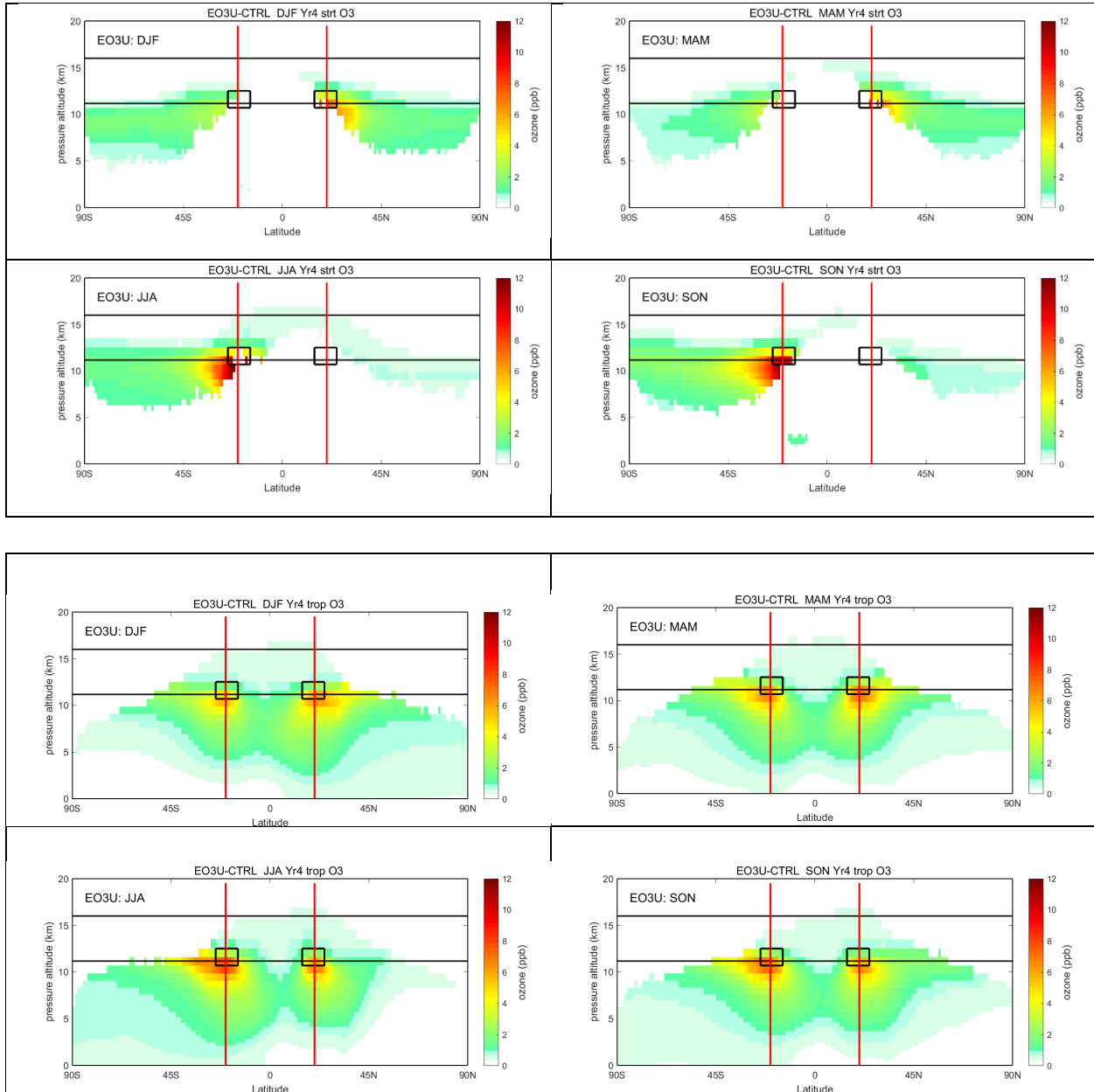


**Figure A9. eO3ste2 perturbation to zonal mean O<sub>3</sub> abundance (ppb) for four seasons (DJF, MAM, JJA, SON), split into stratospheric (top panels) and tropospheric (bottom panels). For methodology, see Figure A1. STE emissions (eO3ste2) occur within the black squares equally in each hemisphere and across all longitudes, see Table 1.**

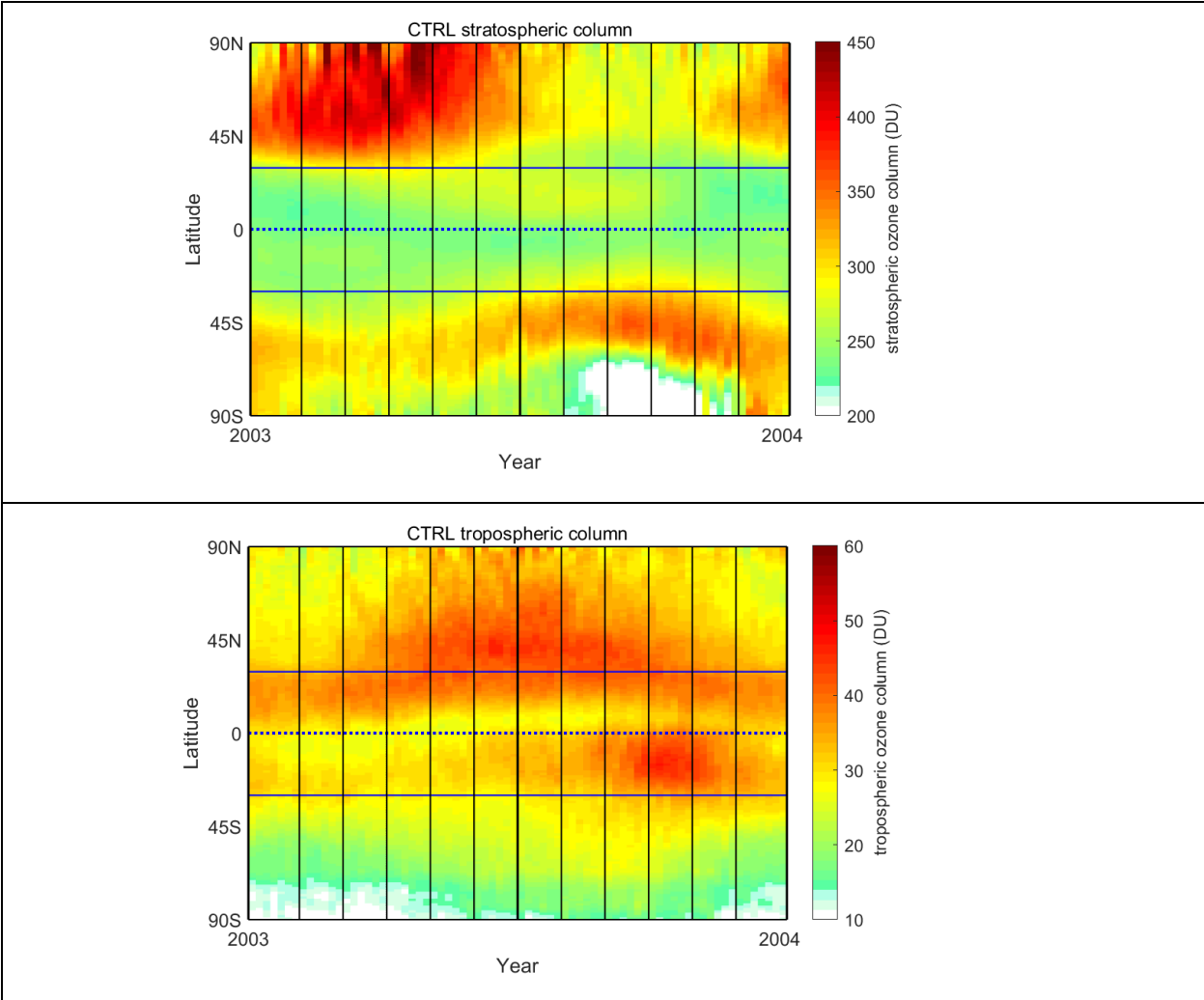


**Figure A10. Stratospheric (top) and tropospheric (bottom) O<sub>3</sub> column (DU) for year 2003 from the control (CTRL) simulation. Columns are a function of latitude and time at 5-day intervals.**

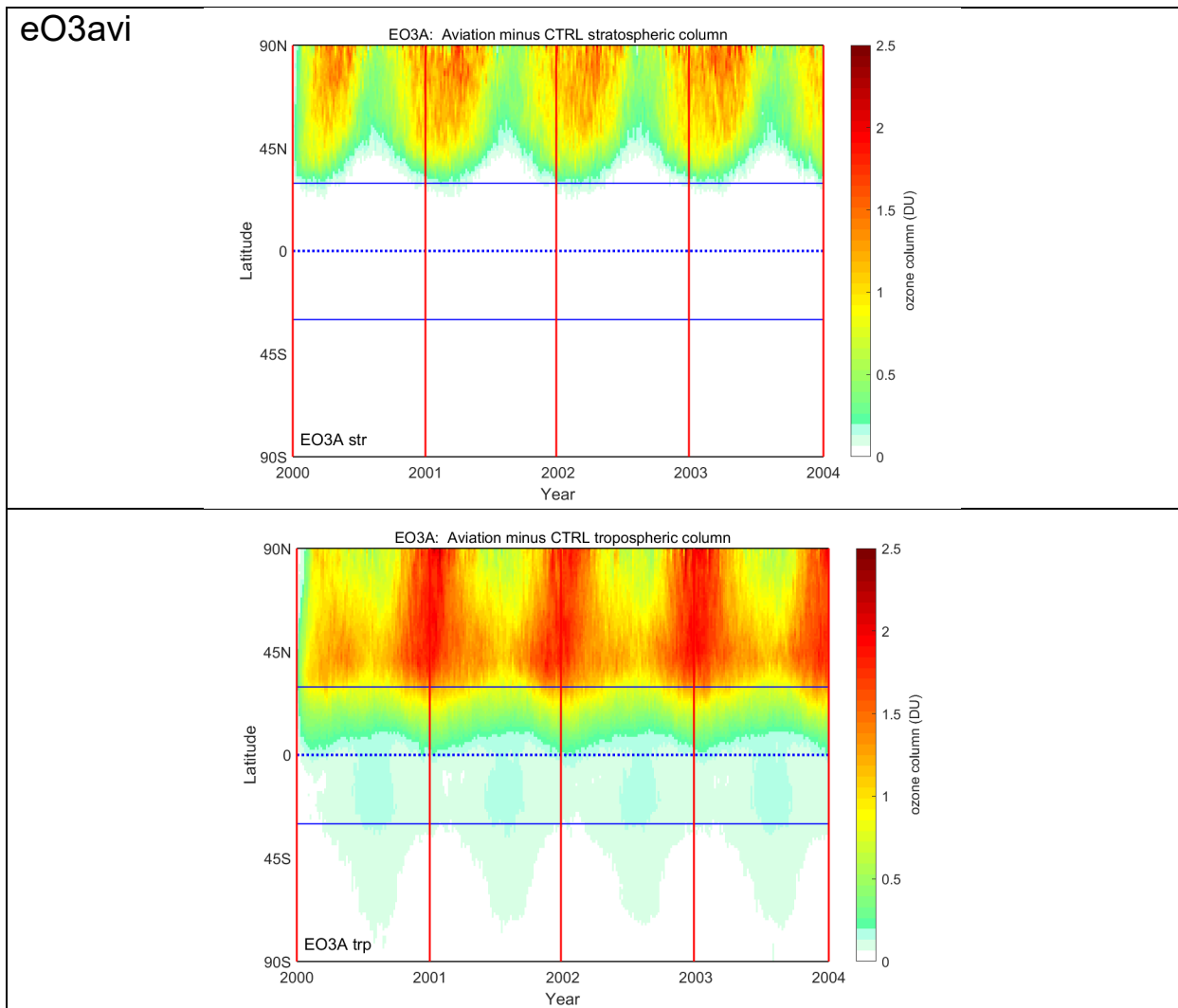


**Figure A11. Ozone column perturbation (DU) for experiment eO3avi (aviation O<sub>3</sub>) as a function of latitude and time (2000.0 to 2004.0) at 5-day intervals for stratosphere (top) and troposphere (bottom).**

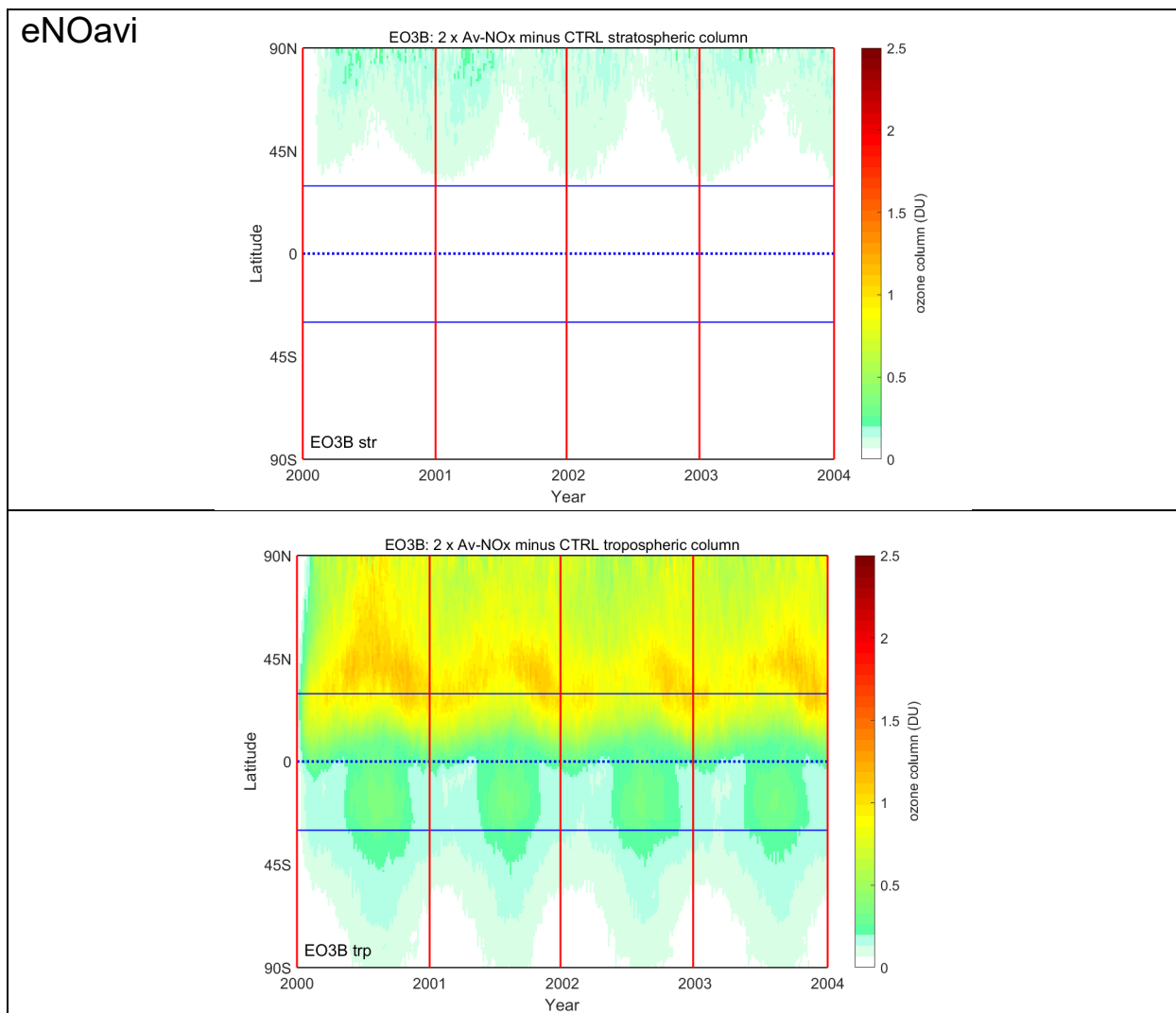


**Figure A12. Ozone column perturbation (DU) for experiment eNOavi (aviation NO<sub>x</sub>) as a function of latitude and time (2000.0 to 2004.0) at 5-day intervals for stratosphere (top) and troposphere (bottom).**

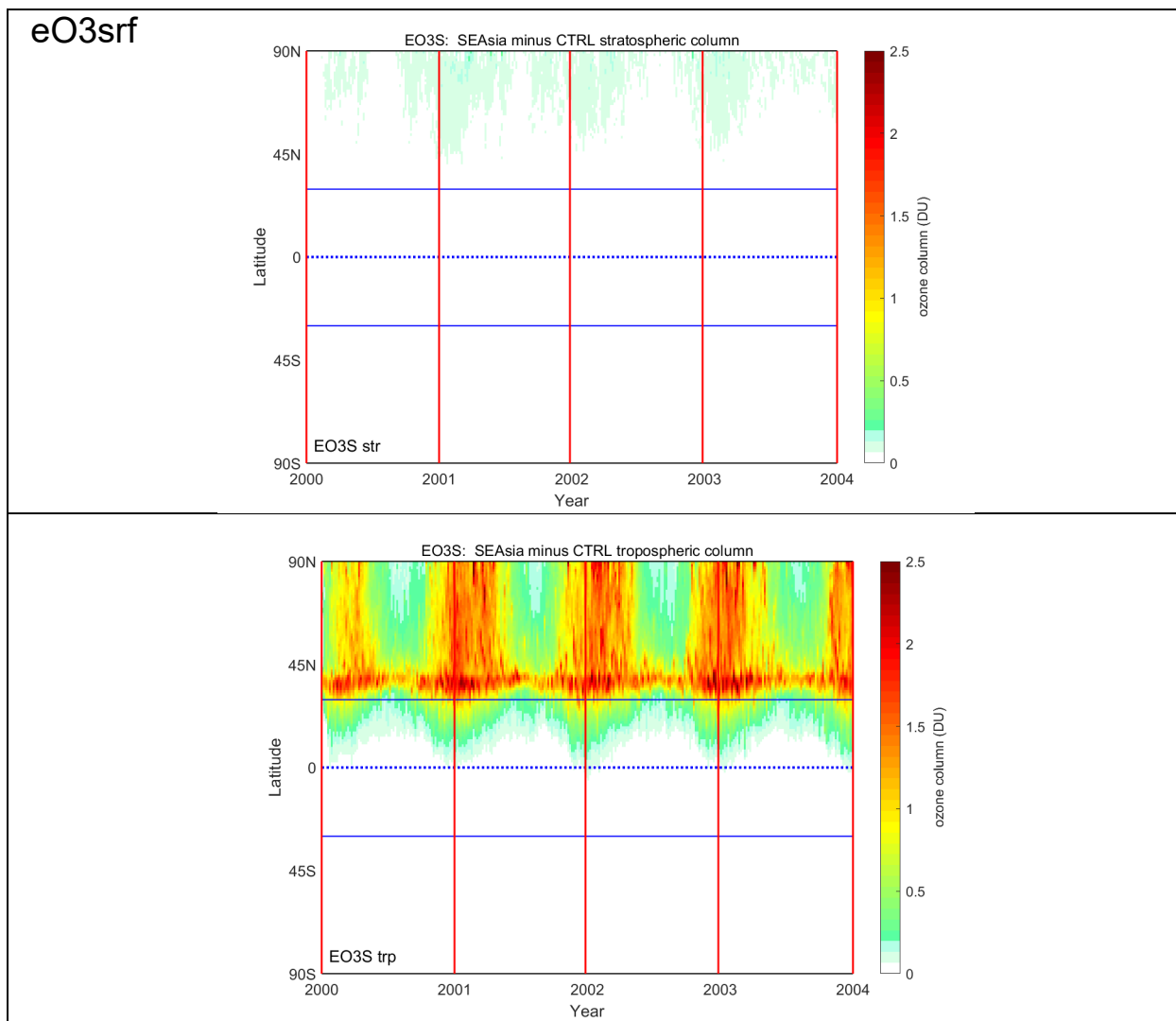


**Figure A13. Ozone column perturbation (DU) for experiment eO3srf (surface O<sub>3</sub>) as a function of latitude and time (2000.0 to 2004.0) at 5-day intervals for stratosphere (top) and troposphere (bottom).**

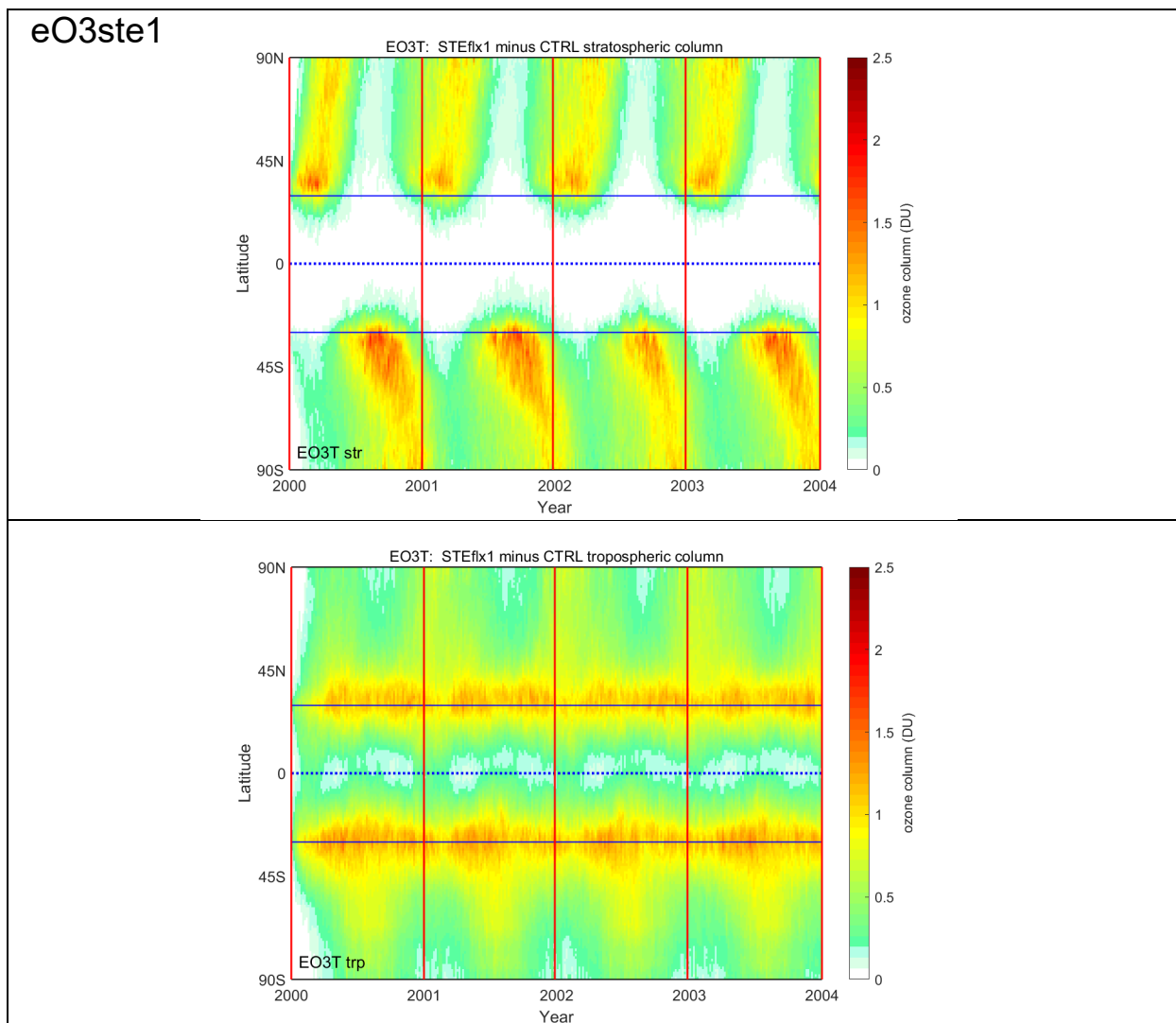


**Figure A14. Ozone column perturbation (DU) for experiment eO3ste1 (1<sup>st</sup> STE O<sub>3</sub>) as a function of latitude and time (2000.0 to 2004.0) at 5-day intervals for stratosphere (top) and troposphere (bottom).**

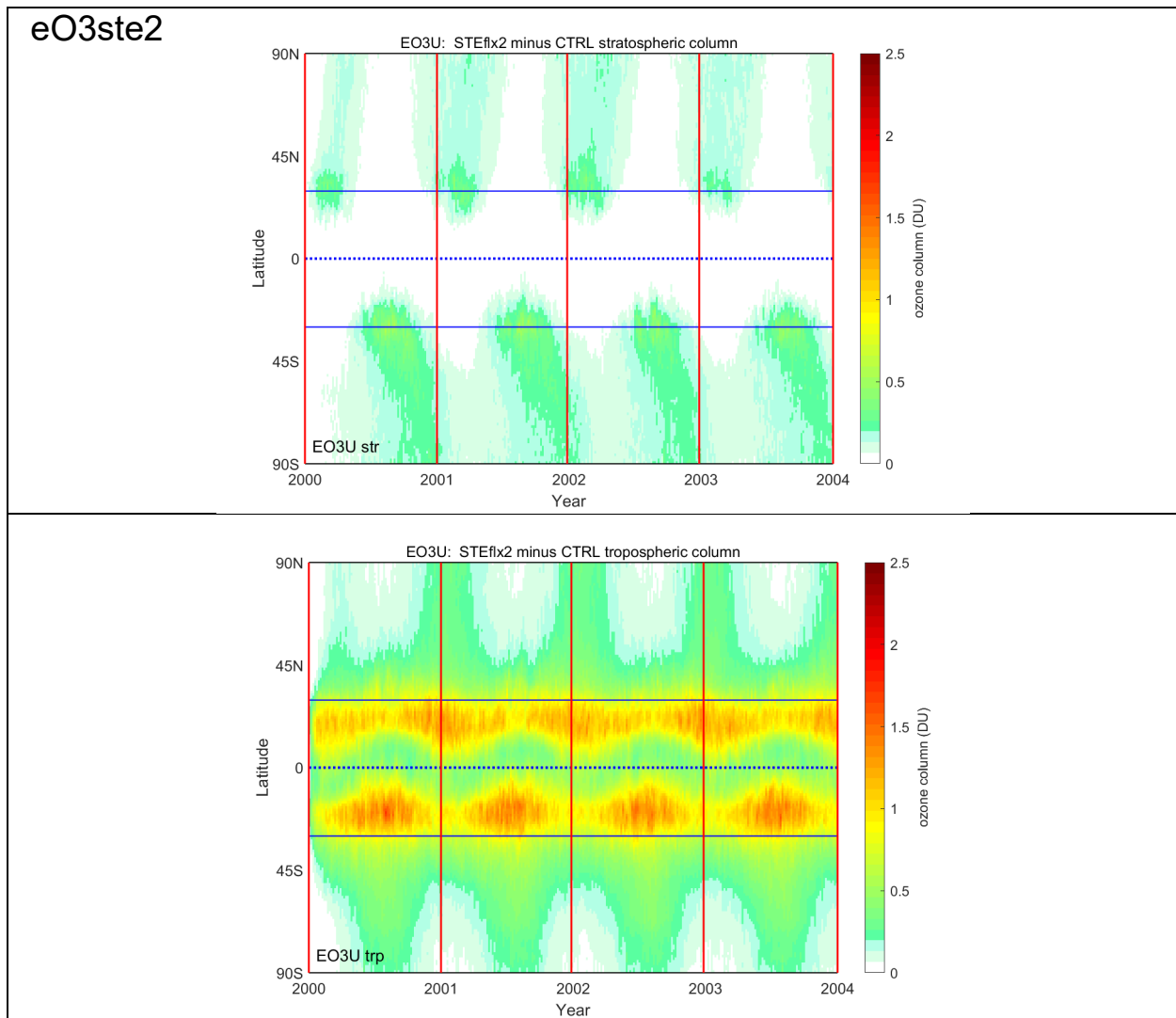


**Figure A15. Ozone column perturbation (DU) for experiment eO3ste2 (2<sup>nd</sup> STE O<sub>3</sub>) as a function of latitude and time (2000.0 to 2004.0) at 5-day intervals for stratosphere (top) and troposphere (bottom).**

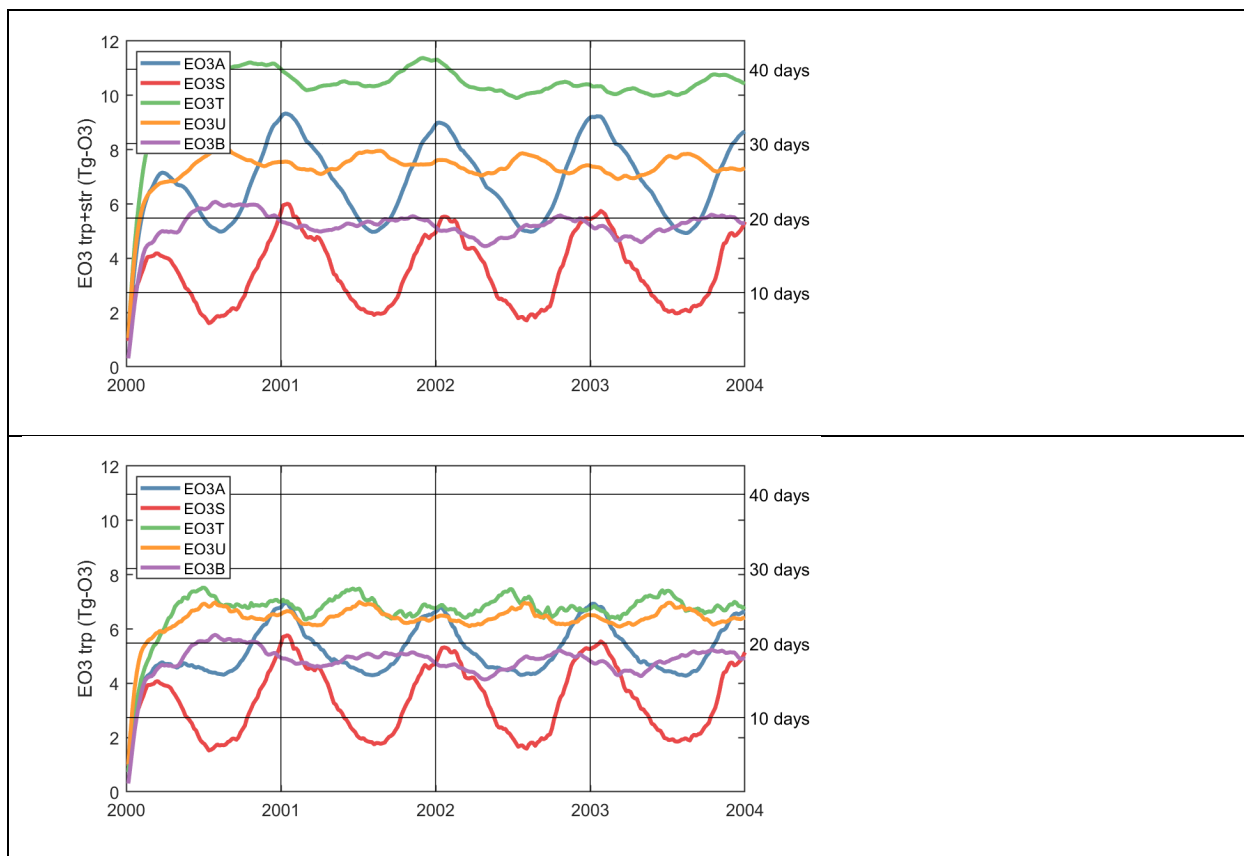


**Figure A16. Total (top) and tropospheric (bottom) burden of excess O<sub>3</sub> (Tg) for the five experiments, showing 5-day intervals for years 2000 through 2003. The spin up in early 2000 is clearly visible. The lifetime scale (days, right axis) is calculated from the emission rate of 100 Tg-O<sub>3</sub> yr<sup>-1</sup> for both tropospheric and total burden, and it does not apply to eNO<sub>avi</sub>. The legend notation is: EO3A = eO3avi; EO3S = eO3srf; EO3T = eO3ste1; EO3U = eO3ste2; EO3B = eNOavi..**

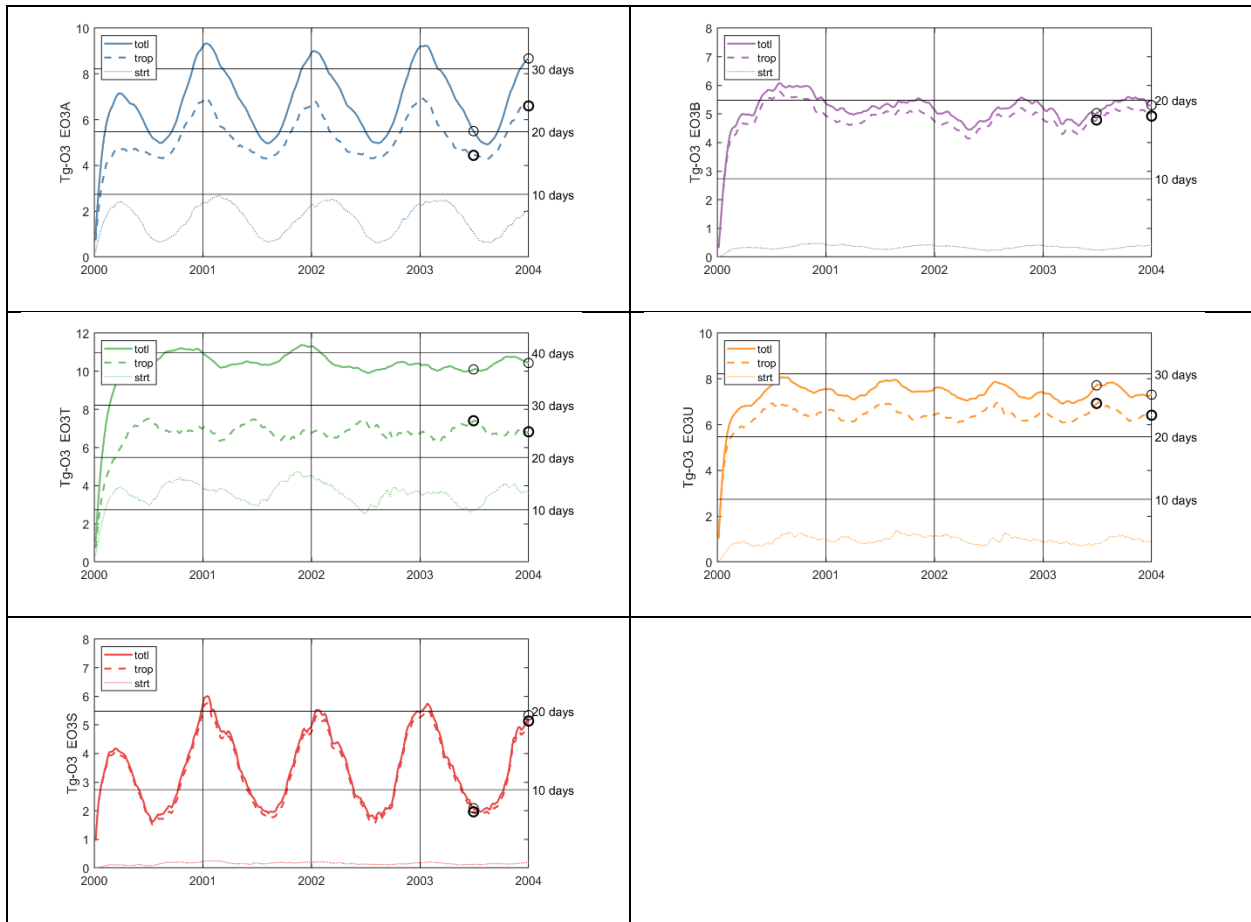


**Figure A17. Burden of excess O<sub>3</sub> (Tg) for the five experiments.** For each experiment, the tropospheric (dashed line), stratospheric (dotted line) and total (solid line) are shown. See Figure A16. The y-axis notation is: EO3A = eO3avi; EO3S = eO3srf; EO3T = eO3ste1; EO3U = eO3ste2; EO3B = eNOavi;

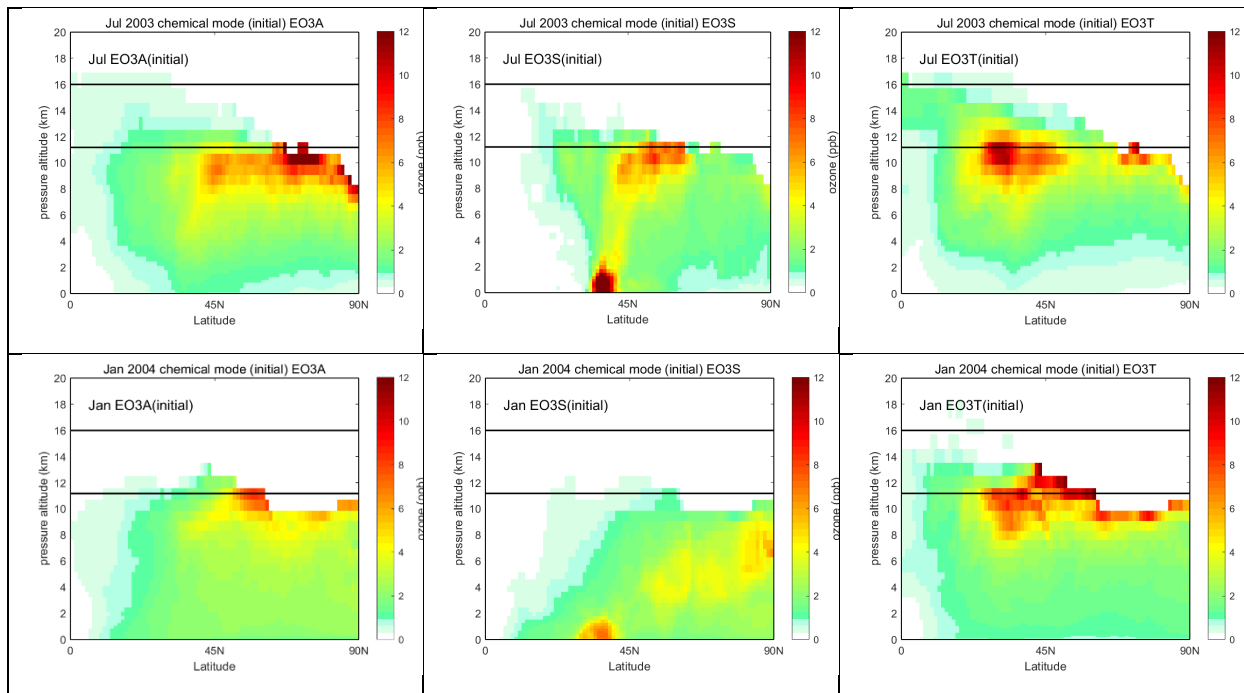


**Figure 18.** Instantaneous patterns of NH tropospheric  $O_3$  perturbation for eO3avi/srf/stel1 at 1 Jul 2003 and 1 Jan 2004. All patterns are scaled to a total of 5 Tg. Figure titles: EO3A = eO3avi; EO3S = eO3srf; EO3T = eO3stel.

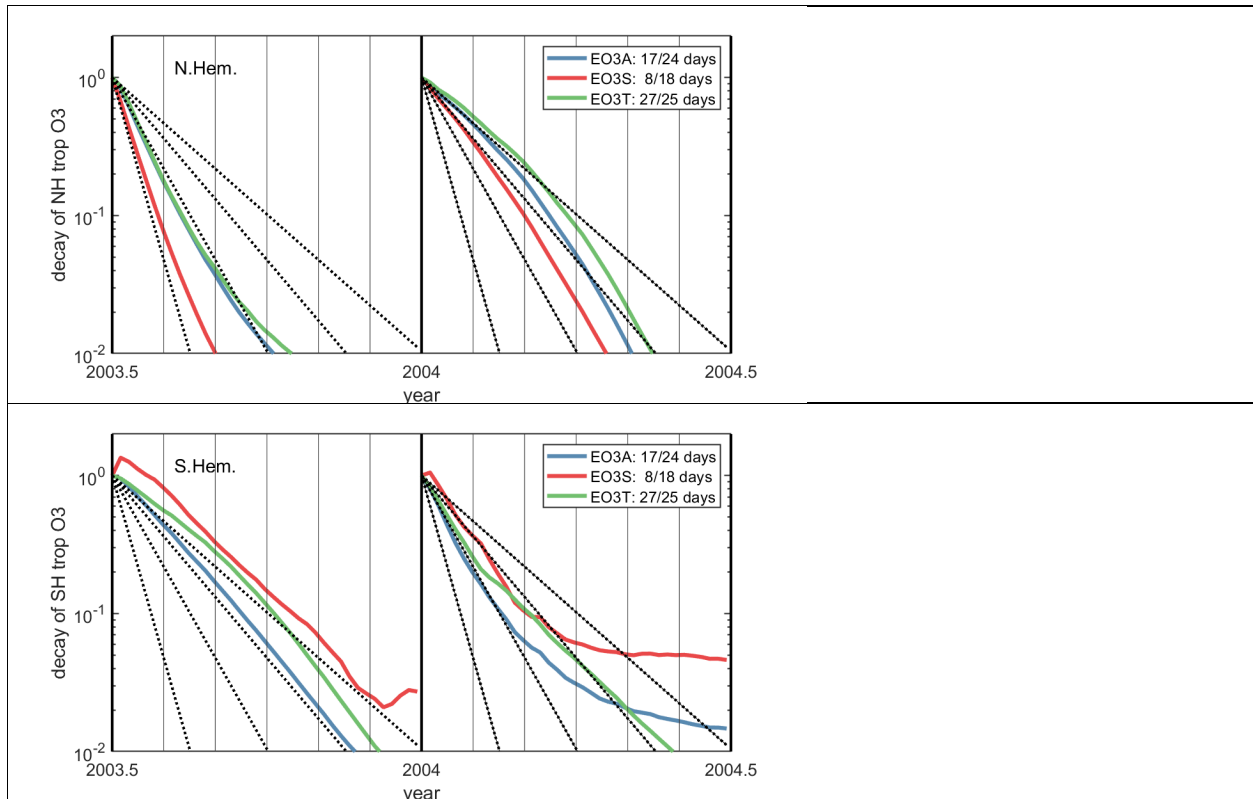


**Figure A19. (top) Decay of northern hemisphere tropospheric O<sub>3</sub> perturbations (Tg) for eO3avi/srf/ste1 rescaled to 1 at the time of cessation of emissions on July 1 (left) and January 1 (right).** Dashed black lines are the same in both panels and show a constant decay of 10- (steepest), 20-, 30- and 40-day e-folds. The legend gives the min-to-max range in steady-state lifetime. Months are marked with vertical lines. (bottom) Same plot for southern hemisphere tropospheric O<sub>3</sub>. The legend notation is: EO3A = eO3avi; EO3S = eO3srf; EO3T = eO3ste1.

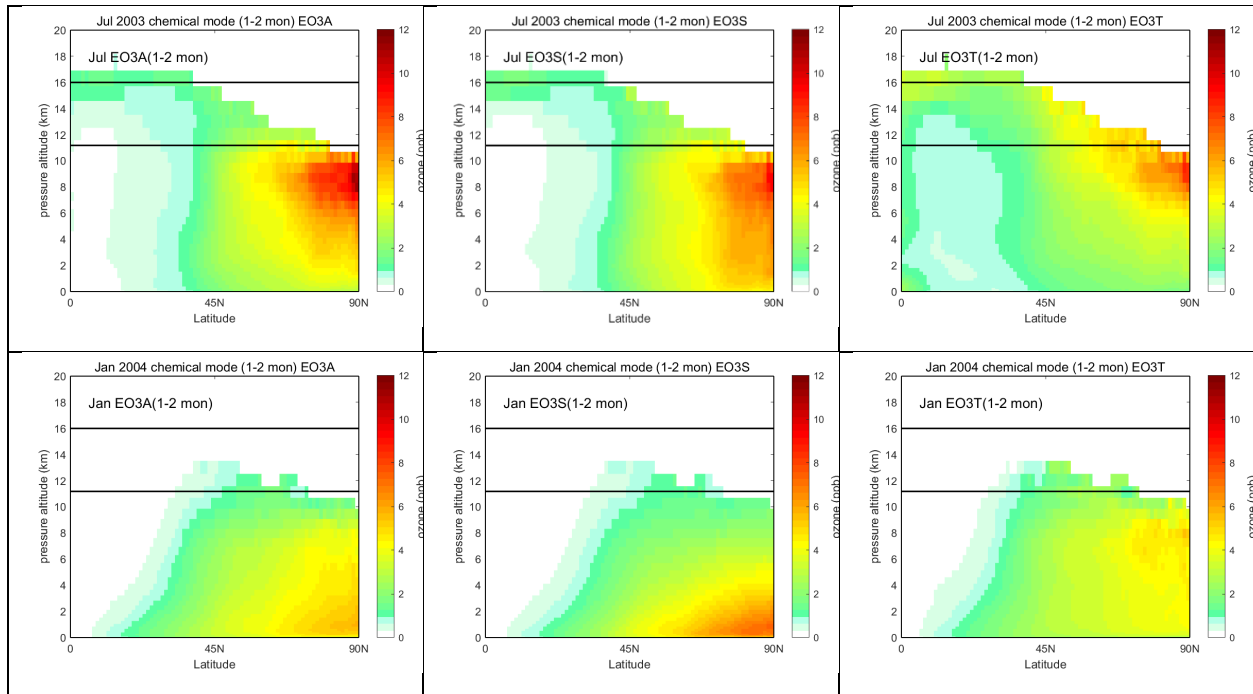


**Figure A20. Chemical mode patterns for the troposphere following decay of eO3avi/srf/stel1 starting at 1 Jul 2003 and 1 Jan 2004. Modes are calculated from averaged NH patterns after 1-2 months decay (days 30-85). All perturbations are scaled to a total NH tropospheric O<sub>3</sub> perturbation of 5 Tg.**

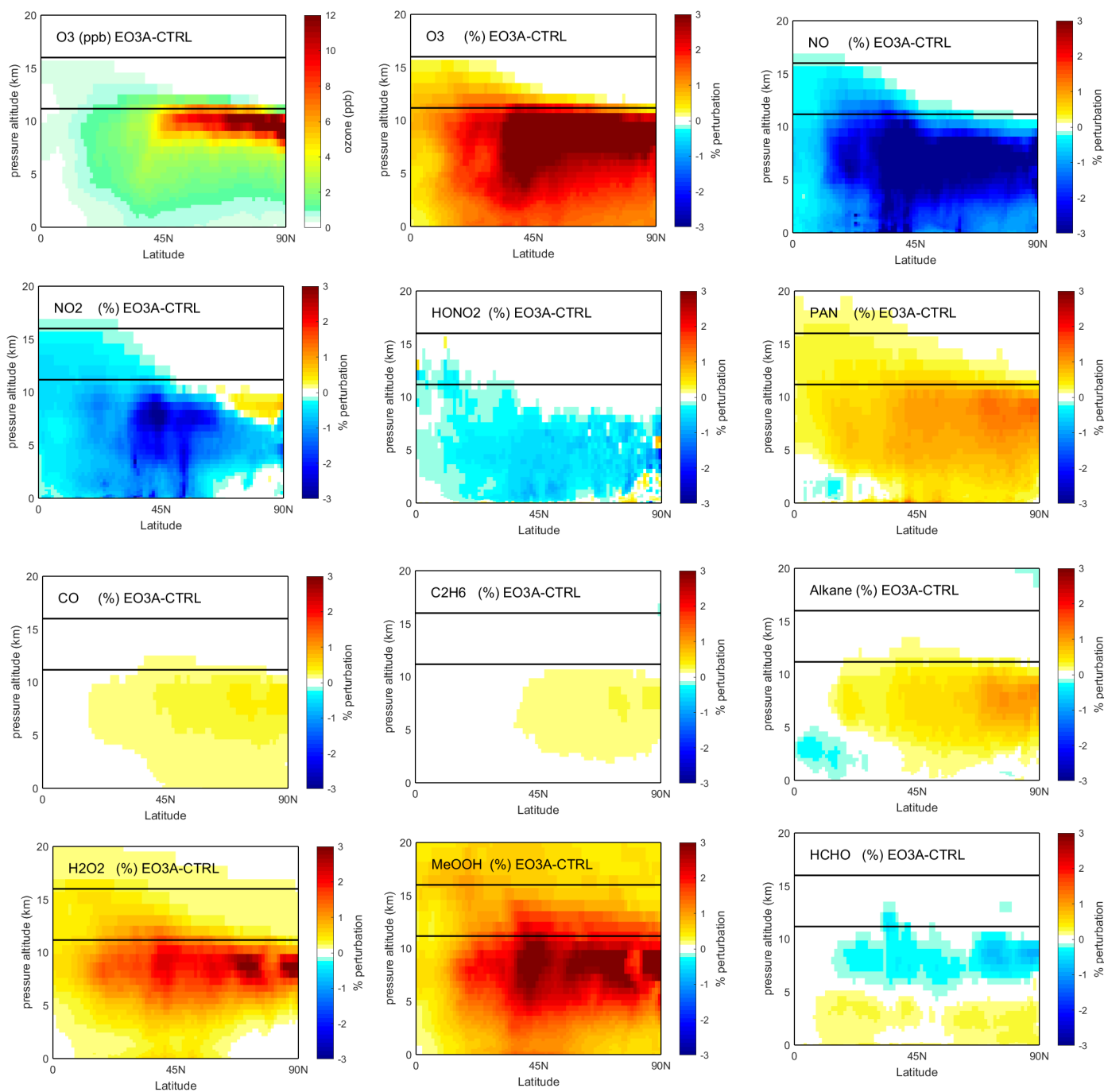


**Figure A21. Latitude-by-altitude plots of the perturbations to key chemical species for the eO3avi (aviation) vs. CTRL on 1 Jul 2003.** The upper-left-corner panel shows the O<sub>3</sub> perturbation in ppb to compare with earlier figures. All other panels, including the 2<sup>nd</sup> O<sub>3</sub> panel are in % difference. Note that the color bar, -3% to +3%, is the same for the eleven relative change panels.